Benthic carbon mineralization on a global scale

Katherina Seiter
Department of Geosciences, University of Bremen, Bremen, Germany

Christian Hensen
Forschungszentrum für Marine Geowissenschaften (GEOMAR), Kiel, Germany

Matthias Zabel
Department of Geosciences, University of Bremen, Bremen, Germany

Received 19 January 2004; revised 18 July 2004; accepted 24 August 2004; published 10 February 2005.

[1] In this study we present a global distribution pattern and budget of the minimum flux of particulate organic carbon to the sea floor ($J_{POC\alpha}$). The estimations are based on regionally specific correlations between the diffusive oxygen flux across the sediment-water interface, the total organic carbon content in surface sediments, and the oxygen concentration in bottom waters. For this, we modified the principal equation of *Cai and Reimers* [1995] as a basic monod reaction rate, applied within 11 regions where in situ measurements of diffusive oxygen uptake exist. By application of the resulting transfer functions to other regions with similar sedimentary conditions and areal interpolation, we calculated a minimum global budget of particulate organic carbon that actually reaches the sea floor of $\sim$0.5 GtC yr^{-1} (>1000 m water depth (wd)), whereas approximately 0.002–0.12 GtC yr^{-1} is buried in the sediments (0.01–0.4% of surface primary production). Despite the fact that our global budget is in good agreement with previous studies, we found conspicuous differences among the distribution patterns of primary production, calculations based on particle trap collections of the POC flux, and $J_{POC\alpha}$ of this study. These deviations, especially located at the southeastern and southwestern Atlantic Ocean, the Greenland and Norwegian Sea and the entire equatorial Pacific Ocean, strongly indicate a considerable influence of lateral particle transport on the vertical link between surface waters and underlying sediments. This observation is supported by sediment trap data. Furthermore, local differences in the availability and quality of the organic matter as well as different transport mechanisms through the water column are discussed.

Citation: Seiter, K., C. Hensen, and M. Zabel (2005), Benthic carbon mineralization on a global scale, *Global Biogeochem. Cycles*, *19*, GB1010, doi:10.1029/2004GB002225.

1. Introduction

[2] From a very simplistic point of view, the marine carbon cycle may be seen as driven by the processes of carbon fixation and release within the water column and geochemical equilibration reactions across the two boundaries, i.e., the atmosphere-water interface and the benthic boundary layer. Unlike the former, the sea floor represents a net sink, where carbon is stored and removed from the cycle for long periods of time. Biogeochemical processes in marine sediments consequently play a key role in understanding the budget of the marine carbon cycle and, ultimately, the global carbon cycle [*Jahnke*, 1996; *Christensen*, 2000; *Wenzhöfer and Glud*, 2002; *Schlitzer*, 2002; *Lasaga and Ohmoto*, 2002; *Archer*, 1996]. General questions frequently discussed are: How much organic carbon reaches the sea floor? Where are the main depot-centers? What are the driving processes of organic carbon accumulation, and which portion is recycled by early diagenetic processes?

[3] Only a small fraction of the primary production settles to the sediment surface. According to *Wollast* [1998], this portion amounts to 1–1.5% of the primary production (PP) in the open ocean, and up to 17% on the upper slopes. Owing to intense microbial degradation in surface sediments, only 0.014% and 0.5–3% of PP are permanently buried in these two regions, respectively. On an ocean-wide scale, the accumulation and burial of organic matter principally reflect the distribution pattern of the primary production. On the basis of local estimates of surface productivity and trap data, several studies [e.g., *Suess*, 1980; *Betzer et al.*, 1984; *Berger et al.*, 1989; *Pace et al.*, 1987; *Schlüter et al.*, 2000; *Antia et al.*, 2001; *Wenzhöfer and Glud*, 2002]

0886-6236/05/2004GB002225$12.00

therefore devised empirical equations to describe the rain rate of particulate organic carbon (POC) as decreasing relative to water depth. Regionally, however, this approach consisting of a simple vertical transport may not be sufficient, since an intense water circulation and strong bottom water currents can cause considerable lateral transport of suspended matter, especially across shelf breaks and down the slopes [*Jahnke et al.*, 1990; *Reimers et al.*, 1992; *Garzoli*, 1993; *Rowe et al.*, 1994; *Peterson et al.*, 1996; *Wollast*, 1998; *Arthur et al.*, 1998; *Hensen et al.*, 2000; *Giraudeau et al.*, 2002; *Mollenhauer et al.*, 2002; *Hensen et al.*, 2003]. Approximately 2.2 GtC are exported to the deep ocean via lateral transport [*Wollast*, 1998]. Furthermore, common empirical equations also do not take into consideration other effects like potential riverine input of organic matter, which can significantly influence the accumulation and burial of organic carbon [*Schlesinger and Melack*, 1981; *Ittekkot*, 1988; *Hedges*, 1992; *Meybeck*, 1993; *Hedges and Keil*, 1995; *Ludwig et al.*, 1996; *Wagner et al.*, 2003]. Additional factors govern the organic carbon rain through the water column and thus decouple the empirical relation between surface primary production and organic carbon flux to the sea floor. Recent studies have corroborated former observations that the composition of particle rain is also of particular importance. According to *Armstrong et al.* [2002] and *Klaas and Archer* [2002], POC fluxes are tightly linked quantitatively to the fluxes of opal and calcite, which, together with lithogenic minerals, function as ballast carriers and, therefore, may exert an influence on the degradation efficiency of POC in the water column. Furthermore, an increasing flux of nonreactive particles to the sea floor reduces the time of exposure to oxygen, thereby enhancing the burial of organic matter [e.g., *Jahnke*, 1996; *Hartnett et al.*, 1998]. Finally, the availability of oxygen in bottom water can affect the preservation of organic matter [e.g., *Betts and Holland*, 1991; *Calvert and Pedersen*, 1992; *Archer and Devol*, 1992; *Cai and Reimers*, 1995].

[4] In general, two approaches are used to quantify the POC flux to the sea floor (J_{POC}). The direct method is based on particle collections by sediment traps. As mentioned before, this approach is susceptible to misinterpretation due to several effects named above. Additionally, the number of such measurements is rather limited. The indirect approach is based on correlations between various proxy parameters. For example, *Jahnke* [1996] has specified and estimated global J_{POC} via the total diffusive benthic oxygen uptake and carbonate corrected organic carbon burial rates. In any case, several previous approaches limited their investigations to the regional variabilities of environmental conditions [e.g., *Jahnke and Jackson*, 1987, 1992; *Cai and Reimers*, 1995; *Christensen*, 2000; *Schlüter et al.*, 2000; *Antia et al.*, 2001; *Sauter et al.*, 2001; *Wenzhöfer and Glud*, 2002] and provided valuable contributions with regard to global approaches.

[5] In our study, we emphasize the key role of the total organic carbon content (TOC) in surface sediments in calculating the flux of particulate organic carbon (J_{POC}), since TOC in surface sediments constitute a key parameter in the control of mineralization processes and the material exchange between the sediment and the ocean water. Therefore TOC is used as proxy parameter representing the most frequently available sedimentary parameter for organic carbon supply to the sea floor. Additionally, TOC is subject to long-term fluctuations, greatly facilitating the evaluation of mean organic carbon input by various vertical and lateral transport processes. For this purpose the regular global TOC distribution pattern published by *Seiter et al.* [2004] can be applied. Since the oxidation of organic matter by dissolved oxygen represents the most important mineralization process, oxygen consumption rates can be utilized for the approximation of the total benthic mineralization rate and hence for a global estimation of the particulate organic carbon flux to the sea floor. Since the database of diffusive oxygen consumption rates (DOU) is restricted to 125 global in situ measurements, we followed the indirect approach of developing specific transfer functions by multiple regression analyses of TOC as a proxy parameter; DOU and the bottom water oxygen concentration served as the rate-limiting parameter [*Archer and Devol*, 1992; *Cai and Reimers*, 1995]. Characterization of typical relationships between these parameters in different benthic provinces enables us to extrapolate these observations to the global ocean. Finally, the resulting distribution pattern of J_{POC} is discussed next to other global studies based particularly on surface productivity and sediment trap data and a rough estimation of the global TOC burial rate is provided.

2. Methods

2.1. Global Database and Data Compilation

2.1.1. Raster Data

2.1.1.1. Total Organic Carbon Content in Surface Sediments (TOC, <5 cm Sediment Depth)

[6] As a basis of TOC distribution on the deep-sea floor, we used the global map of *Seiter et al.* [2004], which is shown in Figure 1a. TOC was used as proxy parameter for the benthic mineralization of organic carbon subsequent to its correlation with the diffusive and total oxygen uptake occurring in specific regions.

[7] The consideration of regional variabilities in intercorrelations of the total organic carbon content (TOC) and the diffusive and total benthic oxygen uptake (DOU, TOU) is based on the discretization of the benthic regime into 33 TOC-based regional provinces (Figure 1b) [*Seiter et al.*, 2004].

[8] As the patterns of primary production differ from those of the TOC content in sea floor sediments, given classifications as published by *Longhurst et al.* [1995] cannot be simply transferred to the benthic regime. *Seiter et al.* [2004] used the content of calcium carbonate and opal in surface sediments, differences in primary production, surface current patterns, water depth, the local riverine and eolian input, and zones of slope instability to define 33 benthic TOC-based regional provinces in the sense of biogeochemical provinces. In reliance on this approach, they presented a new global map of the benthic TOC distribution in a grid resolution of $1^\circ \times 1^\circ$, which is used in this study. The interpolation procedures are based on the geostatistical semivariogram analysis of the kriging method

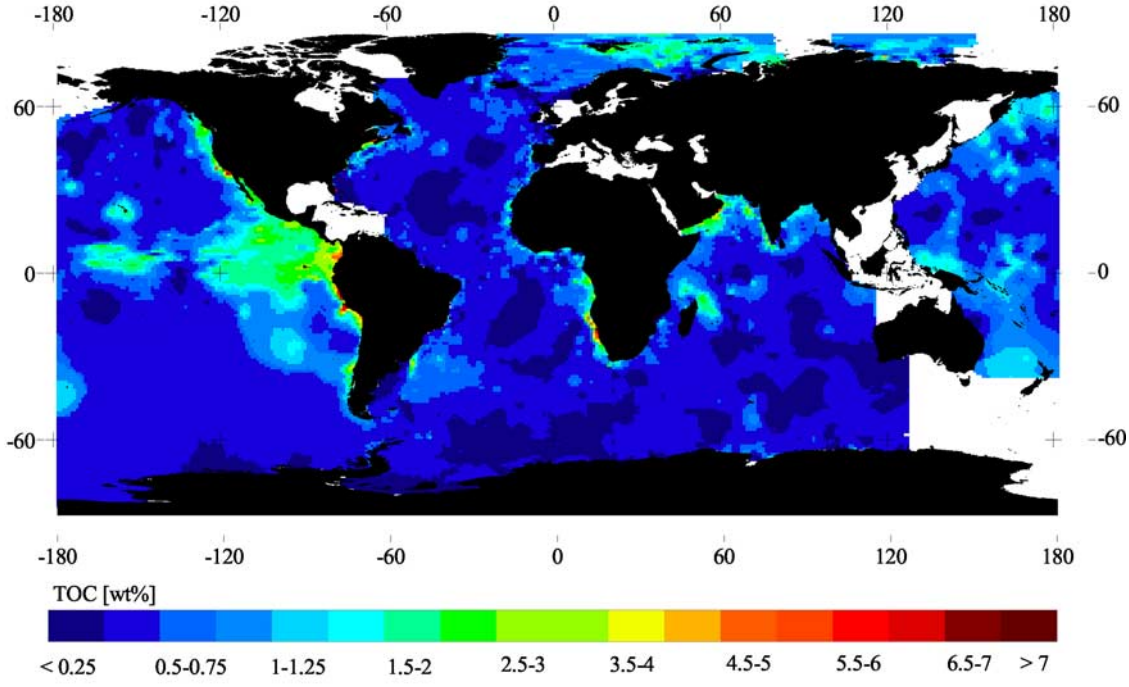

Figure 1a. Global distribution pattern of the total organic carbon content (wt%) in surface sediments (<5 cm sediment depth) [*Seiter et al.*, 2004].

applied to the evaluation of benthic provinces and processing of TOC distribution patterns [*Seiter et al.*, 2004].

2.1.1.2. Empirically Determined Benthic Particulate Organic Carbon Fluxes (J_{POC})

[9] For comparison with the estimation of the particulate flux rates of organic carbon reported in this study, the empirical algorithm of *Antia et al.* [2001] was applied for the latitudes between [65°N, 85°S]. These estimations are based on sediment trap data (equation (1)). For the higher latitudes (>65°N) we used the algorithm of *Schlüter et al.* [2000] to compare our estimations. The pattern was processed with the basic grids of ETOPO5-bathymetry

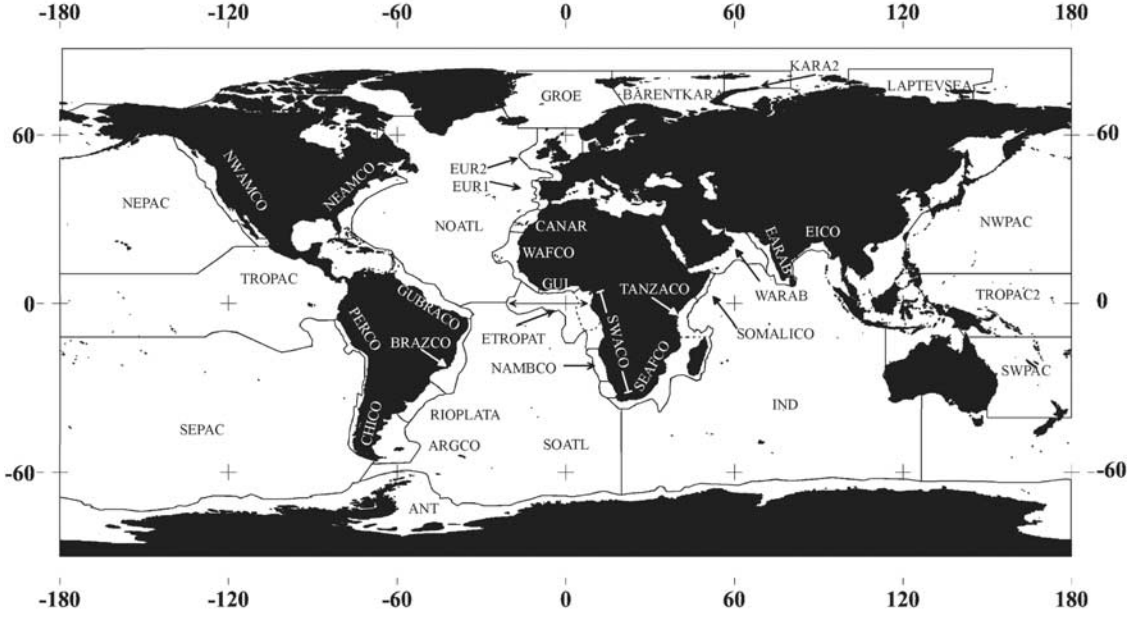

Figure 1b. Updated discretization of the global ocean in 33 benthic TOC-based provinces (TROPAC/TROPAC2; NEPAC/NWPAC; SEPAC/SWPAC; each pair is combined to one province) [*Seiter et al.*, 2004].

Table 1. Parameters, Data Sources, and All References for Data Collection, Compiled for This Study[a]

Parameters	Database	Data Sites/Grid Resolution	Reference
Primary production *Behrenfeld and Falkowski* [1997a, 1997b]	OPD (Oceanographic Productivity Database)	2048 × 1024 binary matrix	*Behrenfeld and Falkowski* [1997a, 1997b] data compilation of primary production (http://marine.rutgers.edu/opp/Production/VPGMRes.html)
Antoine et al. [1996]	JGOFS_France database	2048 × 1024 binary matrix (both exclude ice-cover)	*Antoine et al.* [1996] (http://www.obs-vlfr.fr/jgofs2/modelisation) http://www.obs-vlfr.fr/jgofs/html/html/acces_base.html
Bathymetry ETOPO5	NGDC/WDC MGG (National Geophysical Data Center/World Data Center for Marine Geology and Geophysics, Boulder) USGS (U.S. Geological Survey)	5′ × 5′ matrix	http://www.ngdc.noaa.gov/mgg/global/seltopo.html
Bottom water oxygen concentration	GEOSECS Data IRI/LDEO (Climate Data Library WOCE Data WOD/WOA (World Ocean Database and World Ocean Atlas 1998) Pangaea–Network for Geological and Environmental Data, Literature	1° × 1° matrix based on ~6700 sites	http://ingrid.ldgo.columbia.edu http://www.nodc.noaa.gov/OC5/data_woa.html http://www-ocean.tamu.edu/WOCE/uswoce.html 1° × 1° matrix: this study
Total organic carbon content in surface sediments (<5 cm sediment depth)	Pangaea–Network for Geological and Environmental Data, Literature	1° × 1° matrix based on >5500 surface data sites	1° × 1° matrix [*Seiter et al.*, 2004] http://www.pangaea.de/PangaVista?query=@Ref25653
Organic carbon flux to the sea floor (empirical relation based on *Betzer et al.* [1984], modified after *Antia et al.* [2001])	see Bathymetry and Primary production entries	[80°N, 65°S] 1° × 1° matrix, recalculated	*Antia et al.* [2001]
Trap sites	Pangaea–Network for Geological and Environmental Data, Literature	61 sites	data compilation this study: http://www.pangaea.de/PangaVista?query=@Ref25655
DOU: diffusive oxygen uptake TOU: total oxygen uptake (>1000 m; >550 m water depth for Greenland-Norwegian-Iceland Sea)	Pangaea–Network for Geological and Environmental Data, Literature	number of sites: 125: DOU in situ 39: DOU ex situ 94: TOU in situ	data compilation this study: http://www.pangaea.de/PangaVista?query=@Ref25655
Sedimentation rates (SR), dry bulk density (DBD)	Pangaea–Network for Geological and Environmental Data, Literature	~450 sites	data compilation this study: http://www.pangaea.de/PangaVista?query=@Ref25655

[a]Available from http://www.pangaea.de.

(z) and primary production (PP) after *Antoine et al.* [1996] (Table 1).

$$J_{POC} = c \times PP^a \times z^b, \quad (1)$$

where $c = 0.1$; $a = 1.77$; $b = -0.68$ [*Antia et al.*, 2001] and $c = 1$; $a = 1.873$; $b = -1.172$ [*Schlüter et al.*, 2000].

2.1.1.3. Primary Production (PP)

[10] The calculation of primary production (PP) was derived from *Antoine et al.* [1996]. This model is based on chlorophyll-*a* data acquired by the Coastal Zone Colour Scanner (CZCS, NASA), indicating an annual global budget of 36–43.5 GtC yr^{-1}. Model results were comparable with estimations made by *Behrenfeld and Falkowski* [1997b]. Local differences were caused by higher coastal values estimated by *Behrenfeld and Falkowski* [1997b] and higher estimates along the latitudinal bands between 30°S–50°S and 30°N–80°N. The basin-wide estimates derived from *Behrenfeld and Falkowski* [1997a, 1997b] were lower, whereas the estimates for the higher latitudes (above 60°N) were significantly higher than the corresponding mean values of *Antoine et al.* [1996]. Although there is a general agreement among the different models for particular stations, the estimates after *Antoine et al.* [1996] show a better agreement with measured data [*Antia at al.*, 2001]. Thus we processed the primary production estimates after *Antoine et al.* [1996] in further calculations.

2.1.1.4. Oxygen Concentration in Bottom Water

[11] To evaluate the rate-limiting influence of the oxygen content in overlying bottom water on the mineralization of benthic organic carbon, and thus a potential underestimation of benthic carbon fluxes to the sea floor, the global distribution of the oxygen content in bottom water was gridded. Furthermore, the local influence on oxygen con-

sumption and TOC was investigated. This important point will be discussed in section 3.

[12] In order to compile and interpolate data pertaining to the global distribution pattern of the oxygen concentration in bottom water in a grid resolution of 1° × 1° (compare section 3.1, Figure 2) we combined ~6700 individual bottle data. The main part was queried from the *Electronic Atlas of WOCE Data* [*Schlitzer*, 2000], which provides global ocean observations for the decade between 1988 and 1998. In addition, we used the global hydrographic station data set from the WHP (World Hydrographic Program), obtained from the National Oceanographic Data Center. Two-hundred and thirty-nine individual observations of the Geochemical Ocean Sections study were used, obtained from the Climate Data Library (GEOSECS; IRI/LDEO). Data compilation was supplemented by single datum derived from the literature applying to individual sites. The distribution pattern was calculated by dividing the world oceans into the southern and northern Atlantic Ocean, Pacific Ocean, and Indian Ocean by applying the geostatistical kriging method by semivariogram analyses and interpolation of data [e.g., *Matheron*, 1965].

[13] To avoid artifacts due to the very irregular data distribution, we chose a random selection of 10% of all data to be included in the semivariogram analyses. In each of the oceans, a linear semivariogram could be modeled, indicating that variances steadily increased with increasing distance. The local variance in semivariogram analyses was 250 μmol^2 O_2/L^2 (local standard deviation: 15.8 μmol O_2/L). Gridding errors due to disregarded regional distinctions are assumed to be small, since the local and regional variances were low.

2.1.2. Point Data at Individual Sites

2.1.2.1. Benthic Oxygen Uptake (DOU, TOU)

[14] The data of the benthic oxygen uptake were received from the network for geological and environmental data PANGAEA (www.pangaea.de) and from the literature. The majority of these data refer to measurements of diffusive oxygen uptake in situ (DOU, 125 sites).

[15] As only very few in situ total consumption rates (TOU, 94 sites) are available and apply, at best, to few specific regions, we exclusively used DOU measurements in our calculations (Figure 2, Table 1). In situ TOU data were predominantly used for comparative estimations referring to areas along the continental margin. At the higher latitudes, such as the polar regions, we included ex situ DOU rates (39 sites). Alterations due to the temperature increase during core sampling might be of minor importance compared to decompression effects, since temperature differences between sea floor (−1, 1.3°C) and deck temperatures (<0°C) are generally rather low [*Sauter et al.*, 2001]. Decompression effects increase with water depth and are known to be low in shallow polar seas [*Sauter et al.*, 2001].

[16] For further regression analyses, the corresponding bottom water oxygen content and the measured total organic carbon content in the surface sediment were extracted from the literature and from the network for geological and environmental data PANGAEA (www.pangaea.de), or if no measured data were available from the TOC grid after *Seiter et al.* [2004].

2.1.2.2. Trap Data

[17] A compiled data set based on particle trap data collections made at 61 locations was used (see Figure 10b in section 3.2.2; Table 1). We only considered trap data with a maximum distance to the sea floor of 550 m. At individual sites data were integrated over periods between 61 days and 1 year (annually integrated long-term series).

2.1.2.3. Sedimentation Rates (SR)

[18] In order to estimate the mean burial rates, 450 Holocene sedimentation rates (SR) were compiled. They were calculated by linear age interpolation between the core top and the first tie-point derived from oxygen stable isotope stratigraphy, radiocarbon ages, or as described in the respective literature. The complete data sets of the entire data used in this study can be queried from www.pangaea.de An overview is given in Table 1.

2.2. Regression Analyses

[19] For regression analyses, we correlated DOU with the bottom water oxygen concentration and TOC. The basic approach for these correlations was adapted from *Cai and Reimers* [1995].

[20] The general equation reflects first-order kinetics with regard to the concentration of organic matter, while the oxidant displays a hyperbolic function (monod kinetic) [*Boudreau*, 1997],

$$\frac{-\partial[\mathrm{Ox}]}{\partial t} = -k \times \left([\mathrm{TOC}] \times \frac{[\mathrm{Ox}]}{(K_{\mathrm{ox}} + [\mathrm{Ox}])}\right), \qquad (2)$$

where $\frac{-\partial[\mathrm{Ox}]}{\partial}$ is the time-dependent decay of organic matter per unit area.

[21] [Ox] is the oxygen concentration in overlaying bottom water in mmol m^{-3} and [TOC] is the concentration of organic carbon in surface sediments in wt%. K_{ox} is the saturation constant of the concentration of benthic oxygen in mmol m^{-3}, and k is the rate constant (units of inverse time). The time-dependent decay of organic matter can be replaced by the consumption of oxygen measured in mmol m^{-2} d^{-1}], representing the most important electron acceptor utilized (DOU). The oxygen consumption is also used as an approximation of the total benthic mineralization rate in mmol m^{-2} d^{-1}, calculated by applying constant ratio of organic matter composition (Redfield: C:N:P 106/16/1) and a molar ratio of 106 mol C/138 mol O_2 for the aerobic degradation of organic matter [*Froelich et al.*, 1979]. The modified Redfield ratio according to *Takahashi et al.* [1985] or *Anderson and Sarmiento* [1994] would produce minor changes in the estimated benthic carbon flux that are less than 10%.

[22] Despite the fact that most regression models could be fitted sufficiently with a linear approach in the case of DOU versus TOC, and a first-order rational approach in the case of DOU versus the oxygen concentration in bottom water and versus TOC (equation (2) and *Cai and Reimers* [1995]), provinces displaying an enhanced productivity and reduced DOU were fitted best by means of a logarithmic approach.

We modified equation (2) by the best fit to an empirically derived semilogarithmic relation, which couples DOU with TOC in surface sediments and the concentration of bottom water oxygen concentrations (equation (3)). Additionally, the best regression fits were found, when we considered four constants, K_1, K_2, K_3 and K_{ox}. The influence of the reduced oxygen content in overlaying bottom water was negligible in all regions with $K_{ox} \rightarrow 0$. Thus the reaction is essentially independent of the bottom water oxygen concentration, if this parameter is $\gg K_{ox}$ and the reaction follows first-order kinetics.

$$-\partial\frac{[\mathrm{Ox}]}{\partial t} \approx \mathrm{DOU} = -\frac{[[\ln(\mathrm{TOC}+K_3)]\times K_1 + K_2]\times[\mathrm{BOC}]}{K_{ox}+[\mathrm{BOC}]} \qquad K_{ox}>0 \qquad K_1>0. \tag{3}$$

[23] DOU as well as K_1 and K_2 have the unit mmol m^{-2} d^{-1}, whereas both TOC and K_3 are expressed in the unit wt%, K_{ox} assumes the unit of bottom water oxygen concentration (BOC), i.e., mmol m^{-3}.

[24] To avoid steep gradients between basin and continental margin areas, we included the data of the southern and northern Atlantic and the northeast Pacific basin province, respectively, in the regression analyses. All multiple regression calculations were done by applying the statistics software SPSS® 10.3.

[25] In the relation between TOC and DOU, the degradable fraction of the summary parameter TOC contributes to the depletion of benthic organic matter only (equation (3)). The utilization of the common TOC content will cause the intersection with the axis of the abscissa (TOC_β). Correspondingly, low TOC contents would correlate with a release of oxygen into the bottom water, which stands in contradiction to common observations. To avoid this effect, we defined the following case differentiation: Up to a certain TOC value (TOC_{lim}), we assumed a linear correlation between DOU and TOC (equation 4a); in cases of higher TOC contents as TOC_{lim}, the relation can be described by equation (3), which is then equal to equation (4b). The transition between these two cases is given by the osculation point of a zero-fixed tangent on the function of equation (3). This approach results in the assumption of a linear correlation up to TOC_{lim} (equation 4b; compare section 3.1). TOC_{lim} ranges between 0.32 wt% for the northern and southern Atlantic Ocean and 0.83 wt% for the Pacific Ocean (median global TOC values: 0.6 wt%). The linear relation between DOU and TOC is equivalent to the relation reported by *Cai and Reimers* [1995], if K_{ox} is 0 and applicable to the basin areas where the oxygen concentration of the bottom water is negligible and TOC is generally low (equation (4a)).

$$DOU = [\mathrm{TOC}]\times K \qquad K>0, \mathrm{TOC} < \mathrm{TOC}_{lim} \tag{4a}$$

$$DOU = \frac{[[\ln(\mathrm{TOC}+K_3)]\times K_1 + K_2]\times[\mathrm{BOC}]}{K_{ox}+[\mathrm{BOC}]} \qquad K_{ox}>0, K_1>0, \mathrm{TOC} > \mathrm{TOC}_{lim}. \tag{4b}$$

[26] Estimations of TOU along the continental margin of southwest Africa, the Arabian Sea, the Greenland-Norwegian-Iceland Sea, the continental margin off Chile, and the continental margin off Namibia were derived by an exponential fit. Equation (5) relates the average TOU to the average TOC in the particular provinces.

$$\mathrm{TOU} = \left[K_1 \times \left(\exp^{K_2\times[\mathrm{TOC}]}\right)\right] K_{1,2} > 0. \tag{5}$$

The mean refractory organic carbon content (TOC_β) can be calculated for DOU = 0 and K_{ox} = 0 after equations (6a and 6b).

$$\mathrm{DOU} = 0 = \left[\ln\left(\mathrm{TOC}_\beta + K_3\right)\times K_1 + K_2\right] \tag{6a}$$

$$\mathrm{TOC}_\beta = e^{-\frac{K2}{K1}} - K_3. \tag{6b}$$

The mean burial rate (β in gC m^{-2} yr^{-1}) was calculated by using TOC_β (in %), the sedimentation rate (SR in cm kyr^{-1}), and the dry bulk density (DBD in g cm^{-3}) according to *van Andel et al.* [1975].

$$\beta = 0.1 \times \mathrm{TOC}_\beta \times \mathrm{SR} \times \mathrm{DBD}. \tag{7}$$

The mean DBD and SR values of the different provinces were calculated and used in further data processing and budgeting (Figure 1b).

2.3. Mapping and Budgeting Carbon Fluxes to the Sea Floor

[27] To estimate the global regular distribution of dissolved oxygen uptake (DOU), the regression coefficients, determined by regression fits of DOU (TOU) with TOC and bottom water oxygen concentrations, were applied to the input data grids (TOC, bottom water oxygen content) in the sedimentary provinces, respectively. After merging the particular grids of estimated DOU values, the transition of adjacent provinces was calculated with a moving average of overlapping cells and could hence be smoothed. Nevertheless, the error is assumed to be small due to the avoidance of overlapping areas with high concentration gradients.

[28] The calculation of the global budget of the particulate organic carbon flux to the sea floor ($J_{POC\alpha}$) from DOU grids (section 2.2) and the reference distribution patterns were done by a cell-by-cell calculation with a pseudo-cylindrical equal-area Mollweide projection. Before projection, all grids were recalculated to the same grid extension of 2048 × 1024. Since a projection changes the map area and its geometry, the cells have to be recalculated. Resampling the cells was done by bilinear interpolation of the cell values (Arc View® 3.2a).

3. Results and Discussion

3.1. Regression Analyses and Budgeting

[29] The following section deals with a detailed regression analyses of TOC, flux rates of in situ diffusive oxygen uptake and total benthic oxygen uptake (DOU, TOU), and the oxygen concentration of bottom water. While huge data sets of global TOC and global concentration values of bottom water oxygen are available, oxygen flux measurements are very sparse. Regression fits allows inference of

the benthic oxygen consumption on the basis of TOC in specific provinces. Furthermore, there are many more data applying to DOU than to TOU. Therefore we will first focus on DOU and refer to TOU in local descriptions only. Consequences resulting from this restrictive view will be discussed later (section 3.3).

3.1.1. Influence of Bottom Water Oxygen Concentration on DOU and TOC

[30] The preservation of organic carbon ultimately depends on the time the organic matter is exposed to oxic conditions before it is buried in the surface sediments [*Reimers*, 1989; *Hartnett et al.*, 1998]. Thus, increasing sedimentation rates and decreasing oxygen concentrations in the bottom water along the continental margins favor the preservation of TOC. The global distribution of oxygen in bottom water as shown in Figure 2 clearly illustrates the formation of oxygen-rich deep water to occur mainly in the northern North Atlantic Ocean and the thermohaline circulation pathways. Also remarkable are the oxygen-depleted continental margins, which are especially located along the northwestern continental margin of America, Arabia, and West India.

[31] If the low content of bottom-water oxygen suppresses the mineralization rates on a global scale, this might lead to a strong underestimation of the particulate organic carbon fluxes. As can be seen in Figure 3a, a significant influence of oxygen-depleted bottom water on the benthic respiration rates and the TOC contents for water depths below 1000 m could only be determined for the northeast Pacific region below $\sim$50–70 mmol m^{-3}. Our results therefore confirm the dependencies previously found by *Cai and Reimers* [1995] along the continental margin of northwest America. The TOC content decreases sharply, while the oxygen concentration in the bottom water increases until it reaches nearly 50 mmol m^{-3}. The TOC content remains relatively constant between values of 50 and 125 mmol m^{-3}, indicating several underlying processes. Above 125 mmol m^{-3}, the organic carbon content decreases again, with increasing bottom water oxygen concentration. This correlates with better oxygen conditions and a lower input of organic carbon (Figure 3a). As to be expected for the northeast Pacific Ocean, the highest TOC contents correspond to lowest concentration values of bottom-water oxygen. If an exchange of fresh water constantly supplies high oxygen concentrations to the sediment-water interface, no influence of the oxygen concentration could be observed in the bottom water. Nevertheless, scattering data might result from the seasonal and interannual variations in bottom-water oxygen and the local variations in the sedimentation rates of inorganic components, which are likely to dilute the input of organic carbon. The local importance of the oxygen concentration in the bottom water can be clarified by a comparison between the northeast Pacific Ocean and the southeast Atlantic Ocean (Figures 3a and 3b).

[32] While the low regression coefficient already is indicative of the province-specific relation between TOC and DOU, $K_{ox} \rightarrow 0$ indicates a negligible influence of the concentration of bottom-water oxygen on DOU and TOC within the southeast Atlantic Ocean (Figure 3b). In contrast, the limited availability of oxygen in northeast Pacific bottom water below $\sim$50–70 mmol m^{-3} shows a strong effect on the decay of organic carbon as expressed by an increased K_{ox} (Figure 3a). For all other provinces except the northeast Pacific Ocean, the influence of the oxygen concentration in bottom water on oxygen consumption and preservation of organic matter is seen as negligible. Consequently, the minimum rain of organic carbon down to the sea floor (J_{POC_0}) could be derived from DOU and TOC by a simple two-dimensional log-linear regression, which has been applied to these specific provinces.

3.1.2. TOC Versus DOU (TOU)

[33] It is evident that a simple correlation between TOC and DOU (TOU) does not exist on a global scale [*Jahnke*, 1996] (Figure 4), since regionally variable processes influence the TOC content in surface sediments and the rate of mineralization. The most import processes, which control TOC, are the input, the preservation, and dilution of organic matter by nonreactive and organic components [e.g., *Jahnke*, 1996; *Tyson*, 2001]. Thus fluviatil or eolian input, reactivity, and instability of organic matter are regionally restricted and require more detailed regression analyses for specific areas. For this reason, we used the definition of 33 TOC-based benthic zones as previously identified by *Seiter et al.* [2004].

[34] However, a very similar correlation between individual adjoining zones and similar boundary conditions does not allow any differentiation, for example, to the western and eastern Arabian Sea (WARAB/EARAB) and the central northern Atlantic and southern Atlantic Ocean (NOATL/SOATL). The results of the regression analyses applying to zones for which benthic DOU data were available are shown in Figure 5a (I–XI). Coefficients are listed in Table 2. To achieve better comparability, all regression fits are compiled in Figure 5b.

[35] As shown in Figure 5a (XII), no significant difference in the TOC/DOU relations was obtained between the European continental margin (EUR1) and the combined areas of the Rio de la Plata region and the continental margin off Argentina (RIOPLATA/ARGCO). The same applies to the northwest African continental margin (N-SWACO), the northeast American continental margin (NEAMCO), and the combined areas of the continental margin off northwest America and Brazil (GUBRACO/BRAZCO). Ultimately, 10 types of significantly different TOC/DOU relationships were identified (Figure 5a (I–X), Table 2). They reflect the particular environmental boundary conditions, which can be interpreted as resulting from the differences in the instability and availability of the particulate organic matter (POM). Both properties are closely coupled to the source of POM, which may originate either from surface primary production or terrestrial riverine input, and the residence time of organic matter before burial. The latter also depends on the sedimentation rate and the total sedimentary composition [e.g., *Jahnke*, 1996]. In this context, the transport of POM through the water column, and therefore the water depth itself, has an additional effect of great significance. Accordingly, several recent studies, especially from the eastern equatorial Pacific (TROPAC, Figure 5a (IX)), support the so-called mineral association hypothesis, which means that the accelerated

Table 2. Coefficients for the Functional Relationship Between DOU (TOU), TOC, and Bottom Water Oxygen Content[a]

Fit Number	Province	Log-Linear Decay of First Order (Equation (4a))				Rational Function of Monod Kinetics (Equation (4b))						Tangents	Exponential Decay (Equation (5))			Province Description[b]	Transferred Provinces
		DOU-R^2	K_1	K_2	K_3	DOU-R^2	K_1	K_2	K_{ox}	K_3	K	TOC_{lim}	TOU-R^2	K_1	K_2		
I	WARAB/ EARAB[c]	**0.79**	**12.65**	**−13.22**	**2.76**						-	-	0.65	0.92	1.3	seasonal strong upwelling, high eolian input, high mineralization rates, riverine input and lateral advection[3,4,5,31,55, 57]	EICO
II	N-SWACO	**0.73**	**4.10**	**−3.92**	**2.49**						1.28	0.32	0.32	1.34	0.43	strong estuarine upwelling offshore the Congo River, input of terrigenous organic and lithogenic components, intense downslope transport, bottom lateral transport[2, 6,7,8,29,30,40,54]	SEAFCO, SOMALICO S-SWACO TANZACO
II	NEAMCO	0.55	1.46	0.73	0.5						1.49	0.48	0.94	0.90	0.85	relocation of sediment, intense downslope transport, depotcenter at ∼1000 m offshore, high variability of reactivity and refractory components[9,10]	fit II
II	GUBRACO/ BRAZCO	0.86	4.87	−4.66	2.49						1.28	0.32	-	-	-	strong riverine input of terrestrial lithogenic and refractory organic matter (GUBRACO), alongshore transport, and relocation of sediment [11,60,61,62]	fit II
III	CANAR/ WAFCO	**0.62**	**1.77**	**−0.34**	**1.23**						1.28	0.32	-	-	-	strong bottom currents, high eolian input, large amounts of debris flow, submarine landslides, organic rich mega- turbidites, and meandering channels[12,13,14,15,16,17,40,56]	ETROPAT GUI
IV	RIOPLATA/ ARGCO	**0.73**	**0.49**	**0.86**	**0.08**						1.28	0.32	-	-	-	strong surface currents and bottom water flow, high sedimentary dynamics (downslope and bottom lateral), estuarine upwelling and confluence of Malvinas-Brazil current[18,19,20,21,23,25]	
IV	EUR1[c]	0.63	1.43	−0.3	1.2						1.28	0.32	-	-	-	turbitities, large sand volumes dumped to the abyssal plains, accelerate transport of particles in the water column by aggregation, high alteration grade of organic matter with increasing water depth[16,22,24]	fit IV
V	NOATL/ SOATL[d]	**0.72**	**0.28**	**0.83**	**−0.097**	0.55[e]	1.0	0.92	0.85	0.00	1.28	0.32	DOU = TOU	-	-	oligotroph ocean, less primary production, high mineralization in the water column[27]	IND, EUR2
VI	NAMBCO	**0.92**	**0.95**	**1.21**	**0.11**						1.28	0.32	0.99	1.17	0.57	coastal upwelling, high primary production, intense downslope transport, strong bottom currents and moderate to high oxygen consumption, high burial of organic carbon[6,7,8,28,33,34]	

Table 2. (continued)

Fit Number	Province	Log-Linear Decay of First Order (Equation (4a)) DOU-R^2	K_1	K_2	K_3	Rational Function of Monod Kinetics (Equation (4b)) DOU-R^2	K_1	K_2	K_{ox}	K_3	K	Tangents TOC_{lim}	Exponential Decay (Equation (5)) TOU-R^2	K_1	K_2	Province Description[b]	Transferred Provinces
VII	GROE[f]	**0.88**	**7.91**	**−10.31**	**3.23**						-	-	0.94	0.20	2.10	seasonal high primary production, well-oxygenated bottom water, reduced export of organic carbon = high mineralization in the water column, partial ice-cover, high sediment dynamics (erosion/deposition), terrigenous input variable [1,16,35,36,37,38,41,42,43]	
VIII	LAPTEV SEA[f]	**0.45**	**1.16**	**0.27**	**0.18**						-	-	-	-	-	high riverine input of lithogenic particles, high sediment deposition, estuarine upwelling [39,63]	
IX	TROPAC	**0.58**	**0.72**	**0.52**	**0.19**						0.63	0.83	DOU = TOU	-	-	equatorial upwelling, moderate-high primary production, local resuspension of sediment and sediment deposition, high opal and calcite contents, accelerate transport of organic carbon to the sea floor, bottom water well oxygenated[48,49,50,58]	SEPAC/ SWPAC/ TROPAC2
X	CHICO/ PERCO	**0.89**	**2.86**	**−1.83**	**1.77**						0.91	0.67	0.47	1.73	0.26	high coastal upwelling, less terrigenous input of organic carbon but lithogenic components, high oxygen uptake[46,47,59]	
XI	NEPAC/ NWAMCO[g]	0.88	0.77	0.99	0.03	**0.82**	**1.65**	**1.62**	**96.0**	0.00	1.01	0.70	DOU = TOU	-	-	coastal and estuarine upwelling, high −moderate primary production along the cont. margin, less terrigenous input, coastal depletion of oxygen in bottom waters[44,45,51,52,53]	NWPAC

[a]Regression fits in boldface were used for data processing.

[b]Superscripted numbers denote the following references: 1, *van Bodungen et al.* [1995]; 2, *Duineveld et al.* [1997]; 3, *Witte and Pfannkuche* [2000]; 4, *Ittekkot* [1993]; 5, *Manghnani et al.* [1998]; 6, *Uenzelmann-Neben* [1998]; 7, *Walsh et al.* [1991]; 8, *Zabel and Schulz* [2001]; 9, *Anderson and Sarmiento* [1994]; 10, *Rowe et al.* [1994]; 11, *Tintelnot* [1995]; 12, *Sarnthein et al.* [1982]; 13, *van Camp et al.* [1991]; 14, *Lange et al.* [1998]; 15, *Wynn et al.* [2000]; 16, *Weaver et al.* [2000]; 17, *Freudenthal et al.* [2001, 2002]; 18, *Garzoli* [1993]; 19, *Peterson et al.* [1996]; 20, *Hensen et al.* [2000]; 21, *Hensen et al.* [2003]; 22, *Lohse et al.* [1998]; 23, *Benthien and Mueller* [2000]; 24, *Grutters et al.* [2001]; 25, *Frenz et al.* [2003]; 26, *Curry and Lohmann* [1990]; 27, *Mollenhauer et al.* [2004]; 28, *Mollenhauer et al.* [2002]; 29, *Holtvoeth et al.* [2001]; 30, *Meeuwis and Lutjeharms* [1990]; 31, *Prakash Babu et al.* [1999]; 32, *Bremner and Willis* [1993]; 33, *Bremner* [1983]; 34, *Calvert and Price* [1983]; 35, *Hulth et al.* [1996]; 36, *Schlüter et al.* [2000]; 37, *Sauter et al.* [2001]; 38, *van Raaphorst et al.* [2001]; 39, *Stein and McDonald* [2003]; 40, *Wagner et al.* [2003]; 41, *Peinert et al.* [2001]; 42, *Ritzrau et al.* [2001]; 43, *Hebbeln* [2000]; 44, *Rathburn et al.* [2001]; 45, *Castro et al.* [2001]; 46, *Glud et al.* [1999]; 47, *Hebbeln et al.* [2000]; 48, *Smith et al.* [1997]; 49, *Kawahata and Murayama* [2000]; 50, *Lyle et al.* [2000]; 51, *Jahnke et al.* [1990]; 52, *Archer and Devol* [1992]; 53, *Reimers et al.* [1992]; 54, *Tribovillard et al.* [1996]; 55, *Luff et al.* [2000]; 56, *Meggers et al.* [2002]; 57, *van der Weijden et al.* [1999]; 58, *Murray and Leinen* [1996]; 59, *Lamy et al.* [1998]; 60, *Goni* [2001]; 61, *Ludwig et al.* [1996]; 62, *Ovalle et al.* [1999]; 63, *Lobbes et al.* [2000]; 64, *Ramseier et al.* [1999]. For further references, see text.

[c]For DOU-regression fits, only modeled data based on in situ data were considered (EUR1: *Epping et al.* [2002]; WARAB/EARAB: *Luff et al.* [2000]). TOU-regression fits: based on M33/1 cruise [*Witte and Pfannkuche*, 2000].

[d]Regression fits excluding oxygen consumption rates of: GeoB1708-2 [*Glud et al.*, 1994] located at the Walvis Ridge, OMEX data after *Lohse et al.* [1998].

[e]Regression of the southeast Atlantic Ocean: NOATL/SOATL, NAMBCO, N-SWACO. See Figure 3b.

[f]Regression analyses based on ex situ and in situ data (>550 m wd), excluded data: VP6 and 36_201 [*Sauter et al.*, 2001]. No tangents fit with NOATL/SOATL data.

[g]NEPAC: Three-dimensional regression applied; region includes the continental margin of northwest America (NWAMCO), excluded data: BNTH-3-SBC [*Emerson et al.*, 1985] and Reimers_C-133_BC [*Reimers et al.*,1992]; see Figure 3a.

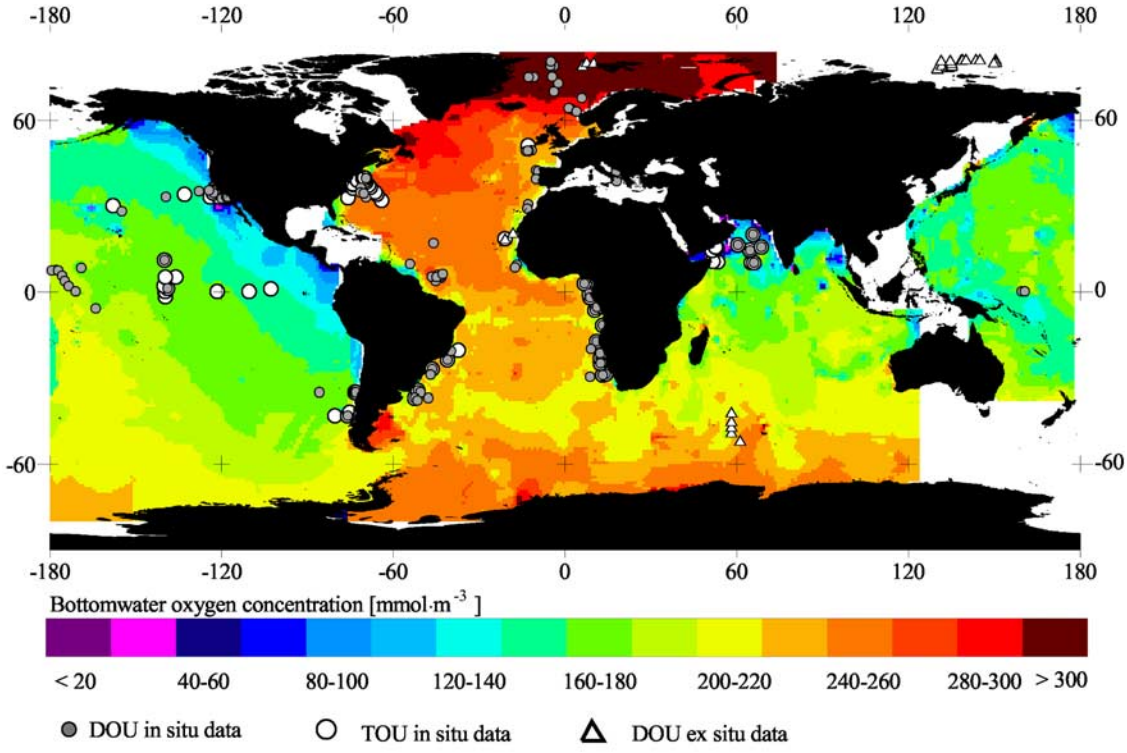

Figure 2. Distribution pattern of the bottom water oxygen concentration measured in mmol m^{-3} and based on ~6700 bottle data (WOCE, GEOSECS). Gray circles: in situ DOU data ; white circles: in situ TOU data ; triangles: ex situ DOU data. Only data used in the regression analyses (wd > 1000 m) are displayed.

export of organic carbon to the sea floor is strongly determined by the presence of ballast minerals like calcite or lithogenic carriers [*Berelson*, 2002; *Armstrong et al.*, 2002; *Klaas and Archer*, 2002]. The steep gradient observed in the subprovinces of the Arabian Sea (WARAB/EARAB; Figures 5a (I) and 5b), indicating high benthic mineralization rates, may therefore have also been caused by the accelerated vertical POM flux. This may be due to the well-known intense eolian dust input from the desert area of the Arabian Peninsula and other Asian sources into this region [*Ittekkot*, 1993; *Haake et al.*, 1993; *Schnetger et al.*, 2000; *Sirocko et al.*, 2000]. This rapid transport probably mediates the deposition of more instable, easily degradable organic carbon.

[36] Other areas in which the intense terrestrial input seems to have great influence may be the polar seas, especially off Svalbard and the region of the western Greenland Sea (see Figure 5a (VII, right)) [*Hulth et al.*, 1996; *Stein and Macdonald*, 2003]. The special relation between DOU and TOC shows a decrease of DOU that is related to the increase of the TOC values (Figure 5a (VII, right)). This behavior may reflect the transport of organic carbon across the slope with an increasing refractory fraction with increasing distance to the coast. Ice coverage and stratification of the water masses and high velocities of the surface current in the northeast polynya reduce the vertical supply of fresh instable organic matter [*Peinert et al.*, 2001; *Ritzrau et al.*, 2001]. Nevertheless, this area is of minor importance for the province budget of POC_{α}, and was therefore not considered in further regression analysis.

[37] For the basin area of the Greenland-Norwegian-Iceland Sea (GROE), the positive relation between TOC and DOU indicates that the overall degradation of organic matter is as high as in the Arabian Sea. Here freshly produced organic matter is rapidly transported from the euphotic zone by aggregate formation during bloom conditions or from lateral sources to the sea floor [*Ritzrau et al.*, 2001] (Figure 5a (I and VII)).

[38] In contrast to the Arabian Sea, the Greenland-Norwegian-Iceland Sea (GROE) is not affected by lithogenic dust. Nevertheless, the importance of terrestrial organic matter and therefore the refractory portion increases progressively towards the east [*Thiede et al.*, 1986; *Hulth et al.*, 1996; *Dowdeswell et al.*, 1998]. However, the high mineralization rates are caused by an intense seasonal production and rapid decay of phytoplankton under well-oxygenated benthic conditions [*Ritzrau et al.*, 2001]. With our interpretation of TOC_{β} (section 2.2, equation (6b)), the highest amounts of refractory organic substance were detected in the Laptev Sea, apparently induced by the intense input of terrestrial material into this area by sediment-laden sea ice [*Eicken*, 2003] and riverine discharges from the rivers Lena and Chatanga (Figure 5a (VIII)).

[39] The continental margin of southwest Africa (NSWACO) holds an intermediate position (Figures 5a (II) and 5b). Both high primary production, fostered by an intense riverine discharge of nutrients, and the extensive input of lithogenic particles from the Ougoue River (0.5°S) and Congo River (6°S) strongly influence this benthic system. Correspondingly, the terrigenous fraction of organic matter is estimated to be at 58–76%, with significant amounts of low reactive mature organic matter [*Wagner et al.*, 2003]. The high content of less reactive and nonreactive particles consequently results in an enhanced preservation of organic matter and slightly lower DOU versus TOC ratios, as compared with other provinces like the Arabian Sea or polar seas.

[40] A system absolutely dominated by marine primary production is the coastal upwelling zone off Namibia (NAMBCO; Figures 5a (VI) and 5b). Here, the tremendous amount of POM produces enhanced sedimentation rates, high TOC contents, and an intense preservation of organic matter. As a result, TOC is positively correlated with DOU but the regression fit has a strong logarithmic shape.

[41] The sedimentary settings are quite different in the western Argentine Basin (RIOPLATA; Figures 5a (IV) and 5b) This region is mainly characterized by an intense lateral particle transport far from the south [*Ewing et al.*, 1964; *Garzoli*, 1993; *Peterson et al.*, 1996; *Hensen et al.*, 2000, 2003], which results in the focusing of few reactive and more lithogenic sediments, especially in the confluence mixing zone of the Malvinas and Brazil current [e.g., *Haese et al.*, 1997; *Romero and Hensen*, 2002]. Pelagic oceans are, in comparison, generally characterized by low sedimentation rates and an intense mineralization already taking place within the water column. As a result, the benthic oxygen uptake in the deep sea is low (NOATL/SOATL, Figures 5a (V) and 5b).

[42] The accuracy of each regional fit function can be demonstrated by calculating DOU from the regression fit (Figure 6) and its subsequent comparison with measured values. The very good regression coefficient of $R = 0.93$ gives evidence of further application of the regression fit functions on the regular TOC grid [*Seiter et al.*, 2004].

[43] Assuming that these 10 types of significantly different TOC/DOU relationships, and the special situation not allowing the limited oxygen concentration in bottom water to be ignored, are representative for the range of all benthic systems in the deep ocean, we are able to estimate benthic POC flux rates on a global scale. This was done by applying the regression analyses to the corresponding provinces and transferring them to regions where no DOU or TOU data exist. As information on the decisive boundary conditions is essential, the main criteria used in this study to identify similar systems were: the existence or absence of riverine input, the oceanographic settings (i.e., type of upwelling, current patterns, trophic situation), the sedimentary settings (i.e., sedimentation rates, sedimentary composition), and the oxygen concentration in bottom water. Thus regions with similar boundary conditions were summarized and their regression types transferred to regions without or only few data. The application of the single regression fits to other provinces is described in Table 2.

3.2. Comparison of Average Rain Rates

3.2.1. Comparisons of Global Budgets

[44] Normally, calculations of the particulate organic carbon fluxes to the sea floor (J_{POC}) are based on sediment trap data [e.g., *Betzer et al.*, 1984; *Berger et al.*, 1989; *Pace et al.*, 1987; *Antia et al.*, 2001]. Apart from this commonly used method, information on benthic oxygen respiration rates can also be used to estimate the amount of organic carbon that accumulates on the sediment surface [e.g., *Jahnke*, 1996], because oxygen uptake is directly correlated with the remineralization of organic matter. Certainly, the portion that is preserved within the sediments cannot be recorded by this approach. Therefore our calculation represents a minimum estimation of the organic carbon rain rate ($J_{POC\alpha}$). Since we only investigated water depths below 1000 m, the influence of anaerobic respiration on $J_{POC\alpha}$ can be assumed to be negligible.

[45] The application of the specific transfer functions to TOC and the concentration grids of bottom-water oxygen results in DOU distribution patterns of $1° \times 1°$ grid resolution. We used the molar ratio of $106C/138O_2$ applicable to the aerobic decay of organic matter (Redfield ratio) after *Froelich et al.* [1979] to convert these values into $J_{POC\alpha}$ (Figure 7), and calculated a global $J_{POC\alpha}$ of ~0.50 GtC yr^{-1} (Table 3). According to *Antoine et al.* [1996], this value would correspond to ~1.6% and 2.5% of the primary production in the deep-sea basins and along continental margins, respectively. The general good accuracy of DOU estimations after applying the regression fits to the regular TOC grid is shown in Figure 8. The very even distribution and the good regression coefficient support our approach and give evidence of the presented distribution pattern. Most of the estimated values have a precision within a factor of 0.5–2, which is in accordance with other studies [*Jahnke*, 1996]. Nevertheless, a few values have higher deviations. Despite the fact that TOC is a good proxy for the organic carbon amount that reaches the sea floor, several factors, which we have already discussed, are also likely to influence the regression. Thus further discretization is needed for better consideration of variable boundary conditions, and a better grid resolution for underlying grids would improve the estimations.

[46] For reasons of comparison, we recalculated the global J_{POC} according to *Antia et al.* [2001]. The estimation of the primary production after *Antoine et al.* [1996] including the ETOPO5 water depth grid J_{POC} yielded a rate of 0.44 GtC yr^{-1} (Table 3). In addition, the approach described by *Jahnke* [1996], which is based on the correlation between the $CaCO_3$-corrected burial rate of organic matter and on the benthic oxygen consumption, was recalculated yielding 0.42 GtC yr^{-1} (60°S–60°N; Table 3, C/O_2 ratio 0.77). In principle, these three fundamentally different approaches produced quite similar results. Figure 9 shows the comparison between the area-integrated $J_{POC\alpha}$ estima-

Table 3. Summary of Calculated Budgets for Each Province[a]

Province	Province Description	Calculated Area (>1000 m wd),[b] km^2	PP,[c] GtC yr^{-1}	PP,[d] GtC yr^{-1}	J_{POC} [*Antia et al.*, 2001],[e] GtC yr^{-1}	JPOC,[f] GtC yr^{-1}	JPOC,[g] GtC yr^{-1}	$J_{POC\alpha}$ (This Study), GtC yr^{-1}	$J_{POC\alpha}$/PP,[c] %	$J_{POC\alpha}$/PP,[d] %
GROE[h]	Greenland Sea	1,963,860	3.94E-01	2.2E-01	2.7E-03	no data	no data	3.66E-03	0.93	1.66
LAPTEV SEA	Laptev Sea	185,066	no data	no data	no data	no data	no data	2.61E-04	no data	no data
KARA2	Kara Sea	15,357	no data	no data	no data	no data	no data	no data	no data	no data
BARENTKARA	Barent Sea and Kara Sea	98,439	no data	no data	no data	no data	no data	no data	no data	no data
NWAMCO	cont. marg. off NW America	1,060,600	3.75E-01	1.82E-01	5.28E-03	4.13E-03	5.29E-03	4.10E-03	1.09	2.25
NEPAC	NE Pacific Ocean	25,753,100	3.17E+00	2.23E+00	2.31E-02	2.10E-02	2.69E-02	3.80E-02	1.20	1.70
NEAMCO	cont. marg. off NE America	544,465	1.05E-01	7.08E-02	1.68E-03	1.21E-03	1.55E-03	1.10E-03	1.05	1.55
SWACO[i]	cont. marg. off SW Africa	1,915,460	6.78E-01	4.05E-01	1.32E-02	5.49E-03	7.05E-03	1.00E-02	1.48	2.47
IND	Indian Ocean	56,511,400	5.79E+00	5.39E+00	7.38E-02	6.86E-02	8.81E-02	8.19E-02	1.42	1.52
NWPAC	NW Pacific Ocean	20,648,700	2.45E+00	1.98E+00	2.26E-02	2.05E-02	2.63E-02	3.70E-02	1.51	1.87
GUI	Guinea Basin	197,487	5.17E-02	3.97E-02	1.07E-03	9.03E-04	1.16E-03	7.50E-04	1.45	1.89
CHICO	cont. marg. off Chile	311,179	1.22E-01	6.69E-02	1.91E-03	3.17E-04	4.07E-04	1.57E-03	1.29	2.35
GUBRACO	cont. marg. off Guyana, Venezuela, Surinam	1,084,600	1.19E-01	1.31E-01	2.81E-03	2.21E-03	2.84E-03	1.80E-03	1.52	1.38
WAFCO	cont. marg. off west Africa	965,796	4.81E-01	2.34E-01	9.46E-03	2.61E-03	3.34E-03	2.30E-03	0.48	0.98
SOATL	southern Atlantic Ocean	37,359,200	4.50E+00	3.77E+00	4.85E-02	3.88E-02	4.98E-02	5.57E-02	1.24	1.48
ARGCO	cont. marg. off Argentina	517,714	6.46E-02	4.21E-02	6.85E-04	5.15E-04	6.62E-04	8.99E-04	1.39	2.13
BRAZCO	cont. marg. off Brazil	1,045,260	9.89E-02	1.21E-01	2.26E-03	1.38E-03	1.77E-03	1.90E-03	1.92	1.57
NOATL	northern Atlantic Ocean	27,585,100	4.57E+00	2.95E+00	4.09E-02	3.38E-02	4.34E-02	3.95E-02	0.86	1.34
CANAR	Canary Islands area	422,511	7.61E-02	5.11E-02	1.12E-03	7.56E-04	9.70E-04	1.01E-03	1.33	1.98
EUR1	southern European cont. marg.	206,535	5.11E-02	2.73E-02	6.29E-04	3.21E-04	4.11E-04	4.75E-04	0.93	1.74
EARAB	eastern Arabian Sea	342,651	6.07E-02	6.95E-02	2.64E-03	1.54E-03	1.97E-03	4.47E-03	7.36	6.43
EUR2	northern European cont. marg.	378,057	1.18E-01	5.11E-02	1.27E-03	6.58E-04	8.44E-04	6.26E-04	0.53	1.22
WARAB	western Arabian Sea	1,887,130	5.48E-01	4.81E-01	1.76E-02	5.52E-03	7.08E-03	2.23E-02	4.07	4.64
RIOPLATA	Rio de la Plata	416,217	7.20E-02	4.83E-02	9.88E-04	9.72E-04	1.25E-03	1.07E-03	1.49	2.22
PERCO	cont. marg. off Peru	393,400	1.36E-01	8.25E-02	2.66E-03	1.22E-03	1.56E-03	3.23E-03	2.37	3.91
TROPAC	eastern tropical Pacific	30,307,900	3.19E+00	3.84E+00	5.95E-02	5.01E-02	6.43E-02	7.10E-02	2.22	1.85
TROPAC2	western tropical Pacific	11,740,600	7.63E-01	1.25E+00	1.94E-02	1.04E-02	1.34E-02	1.87E-02	2.45	1.50
SEPAC	SE Pacific Ocean	53,018,800	5.31E+00	4.15E+00	4.58E-02	3.20E-02	4.10E-02	5.90E-02	1.11	1.42
SWPAC	SW Pacific Ocean	8,297,580	9.26E-01	7.90E-01	1.33E-02	7.99E-03	1.03E-02	1.40E-02	1.51	1.77
SEAFCO	cont. marg. off SE Africa	2,086,590	2.45E-01	2.28E-01	4.46E-03	3.95E-03	5.07E-03	3.67E-03	1.50	1.61
NAMBCO	cont. marg. off Namibia	367,829	9.72E-02	4.88E-02	1.68E-03	6.81E-04	8.74E-04	2.04E-03	2.10	4.18
EICO	cont. margin off E-India	183,324	3.01E-02	3.73E-02	1.54E-03	6.46E-04	8.29E-04	1.71E-03	5.68	4.59
ETROPAT	East equatorial Atlantic	3,843,120	7.90E-01	6.11E-01	1.40E-02	7.25E-03	9.30E-03	9.79E-03	1.24	1.60
TANZACO	cont. marg. off Tanzania	858,792	1.93E-01	2.34E-01	2.60E-03	3.70E-03	4.74E-03	2.57E-03	1.33	1.10
SOMALICO	cont. marg. off Somalia	183,718	4.15E-02	3.88E-02	1.21E-03	4.92E-04	6.31E-04	5.27E-04	1.27	1.36
ANT (area <65°S)	all areas >65°N	4,017,892	1.43E-01	3.97E-01	5.38E-03	no data	no data	5.29E-03	3.69	1.33
Sum		296,347,601	3.71E+01	3.12E+01	4.44E-01	3.30E-01	4.23E-01	5.0E-01	1.40	1.65

[a]Projection: Mollweide, center: zero meridian, all calculations >1000 m water depth, GROE: >550 m water depth. Read 3.94E-01 as 3.94×10^{1}.
[b]Average calculated cell area (>1000 m water depth).
[c]Primary production after *Behrenfeld and Falkowski* [1997a, 1997b].
[d]Primary production after *Antoine et al.* [1996].
[e]J_{POC} after *Antia et al.* [2001] are based on primary production after *Antoine et al.* [1996] and water depth (wd) from ETOPO5.
[f]J_{POC} recalculated after *Jahnke* [1996] from a global oxygen consumption grid with a C:O_2 ratio of 0.6 as described by *Jahnke* [1996].
[g]J_{POC} recalculated after *Jahnke* [1996] with a C:O_2 ratio of 0.77 based on this study.
[h]J_{POC} recalculated after *Schlüter et al.* [2000] instead of *Antia et al.* [2001] for GROE; wd >550 m.
[i]All budgets including NAMBCO corrected in global budget and area.

Table 4. Summary of Mean Flux Rates for All Provinces[a]

Province	PP,[b] gC m^{-2} yr^{-1}	PP,[c] gC m^{-2} yr^{-1}	JPOC,[d] gC m^{-2} yr^{-1}	J_{POC} C/O_2:0.6,[e] gC m^{-2} yr^{-1}	J_{POC} C/O_2:0.77,[f] gC m^{-2} yr^{-1}	$J_{POC}\alpha$ This Study, gC m^{-2} yr^{-1}	TOC,[g] wt%	BOC This Study,[h] mmol m^{-3}
GROE[i]	201	112	1.37	no data	no data	1.86	0.72	310
LAPTEV SEA	no data	no data	no data	no data	no data	1.41	0.97	316
KARA2	no data	no data	no data	no data	no data	no data	no data	202
BARENTKARA	no data	no data	no data	no data	no data	no data	no data	275
NWAMCO	354	172	4.97	3.89	4.99	3.87	1.56	103
NEPAC	123	87	0.90	0.81	1.04	1.48	0.44	154
NEAMCO	193	130	3.08	2.22	2.85	2.02	0.65	228
SWACO[j]	354	211	6.91	2.87	3.68	5.22	1.22	206
IND	102	95	1.31	1.21	1.56	1.45	0.35	203
NWPAC	119	96	1.10	0.99	1.27	1.79	0.58	163
GUI	262	201	5.42	4.57	5.87	3.80	1.00	214
CHICO	391	215	6.14	1.02	1.31	5.05	1.45	192
GUBRACO	109	121	2.59	2.04	2.62	1.66	0.43	207
WAFCO	498	243	9.79	2.70	3.46	2.38	0.64	212
SOATL	120	101	1.30	1.04	1.33	1.49	0.35	231
ARGCO	125	81	1.32	1.00	1.28	1.74	0.38	249
BRAZCO	95	116	2.16	1.32	1.69	1.82	0.54	219
NOATL	166	107	1.48	1.23	1.57	1.43	0.36	257
CANAR	180	121	2.65	1.79	2.30	2.39	0.62	213
EUR1	247	132	3.05	1.55	1.99	2.30	0.80	223
EARAB	177	203	7.70	4.49	5.76	13.05	1.48	93
EUR2	311	135	3.35	1.74	2.23	1.66	0.46	249
WARAB	291	255	9.32	2.92	3.75	11.82	1.36	100
RIOPLATA	173	116	2.37	2.33	3.00	2.57	0.94	202
PERCO	346	210	6.76	3.09	3.96	8.21	3.82	130
TROPAC	105	127	1.96	1.65	2.12	2.34	1.22	160
TROPAC2	65	106	1.65	0.89	1.14	1.59	0.76	158
SEPAC	100	78	0.86	0.60	0.77	1.11	0.49	190
SWPAC	112	95	1.60	0.96	1.24	1.69	0.82	172
SEAFCO	118	109	2.14	1.89	2.43	1.76	0.50	194
NAMBCO	264	133	4.55	1.85	2.38	5.55	1.87	191
EICO	164	203	8.42	3.52	4.52	9.33	1.12	107
ETROPAT	206	159	3.66	1.89	2.42	2.55	0.64	233
TANZACO	224	273	4.30	4.30	5.52	2.99	1.05	191
SOMALICO	226	211	6.58	2.68	3.43	2.87	0.71	186
ANT (<65°S)	36	99	1.34	no data	no data	1.32	0.32	234

[a]All calculations corresponds to water depth >1000 m; GROE: water depth >550 m.
[b]Primary production after *Behrenfeld and Falkowski* [1997a, 1997b].
[c]Primary production after *Antoine et al.* [1996].
[d]Mean J_{POC} recalculated after *Antia et al.* [2001] is based on primary production after *Antoine et al.* [1996] and water depth from ETOPO5.
[e]Mean J_{POC} recalculated after *Jahnke* [1996] from a global oxygen consumption grid with a $C:O_2$ ratio of 0.6 as described by *Jahnke* [1996].
[f]Mean J_{POC} recalculated after *Jahnke* [1996] with a $C:O_2$ ratio of 0.77 based on this study.
[g]Mean TOC values recalculated from global TOC grid after *Seiter et al.* [2004].
[h]Mean BOC is bottom water oxygen content values queried from the grid, this study.
[i]Mean J_{POC} values for GROE recalculated after *Schlüter et al.* [2000].
[j]SWACO: all mean values calculated including NAMBCO.

tions of this study and results calculated by using the method described by *Antia et al.* [2001]. The latter represents the primary production distribution patterns in principle. Only provinces with a significant influence (of $>2 \times 10^{-3}$ GtC yr^{-1}) of the global balance (83.5°N, 85°S) are depicted. Together, these represent about 95% of the global ocean J_{POC}. The calculated budgets within the benthic provinces are summarized in Table 3.

[47] As was to be expected, the highest mean flux rates were calculated for the main upwelling areas off Namibia, Chile, Peru, and the Arabian Sea, areas that are characterized by high organic carbon rain rates to the seafloor and high mineralization rates. While high fluxes were estimated for the central Chile margin, the adjacent northern region was dominated by low fluxes. There was a huge terrigenous sediment supply along the Chilean margin showing an expanding pattern, accompanied by an increasing precipitation southward. Along the Chilean margin, the latitudinal pattern of annual primary production also revealed increasing values towards the south (CZCS data), accounting for an enhanced transport of carbon to the sea floor [*Lamy et al.*, 1998; *Hebbeln et al.*, 2000]. The Chilean topography is marked by a steep rise from sea level to >6000 m of the Andes within 200 km distance from the coast. North of 27°S, the trench reaches its greatest depth of 8000 m below sea level. Here, in contrast to the southern area, the terrigenous input and thus the filling of the trench is very low but mineralization of organic matter in the deep-water column is high.

[48] However, despite the general good agreement of our results with the estimates obtained from the sediment trap data, the primary production, and water depth, conspicuous

Table 5. Summary of Trap Data

Longitude[a]	Latitude[b]	Trap Number	Trap	wd, m	Trap Depth Above Bottom, m	$J_{POC\ Trap}$,[c] gC m^{-2} yr^{-1}	$J_{POC\alpha}$,[d] gC m^{-2} yr^{-1}	$J_{POC\alpha}/J_{POCTrap}$, %	J_{POC},[e] gC m^{-2} yr^{-1}	Editor	Start Date Trap	End Date Trap	Comment[f]
−151.0000	15.0000	1	P1	5792	210	0.24	1.41	578	0.74	*Honjo et al.* [1982]; *Francois et al.* [1995]	01.09.78	01.11.78	[x]
−145.0000	50.0000	2	PAPA	4240	386	2.19	2.19	100	1.07	*Wong et al.* [1999]; *Francois et al.* [1995]	23.09.82	16.05.94	interannual variations
−140.0000	11.0333	3	MANOP_ S	4620	10	0.20	3.29	1613	1.09	*Emerson et al.* [1985]	10.06.80	13.10.81	[x]
−139.7500	−1.9500	4	EqPac 92	3593	0	1.30	1.58	122	2.55	*Honjo et al.* [1995]	annual		
−138.9317	1.0555	5	MANOP_C3	4450	530	1.69	1.10	65	2.20	*Dymond et al.* [1992]	01.05.85		
−138.0000	49.0000	6	PC	4008	508	2.17	1.60	74	1.10	*Francois et al.* [1995]	annual		
−127.7350	49.1183	7	IOS_trap_O5	1978	78	3.21	5.03	157	7.72	*Peña et al.* [1996, *1999*,2000]	03.10.95	29.03.96	water depth from ETOPO 5
−127.7350	49.1183	8	IOS_trap_O6	1978	78	4.44	5.03	113	7.72	*Peña et al.* [1996, 1999, 2000]	14.04.96	01.09.96	water depth from ETOPO 5
−127.7000	39.5000	9	MFZ-4	4356	571	1.44	1.93	134	1.04	*Dymond and Lyle* [1994]; *Ragueneau et al.* [2000]	annual		
−127.7000	39.5000	10	MFZ-11	4230	445	0.95	1.93	203	1.04	*Dymond et al.* [1992]	annual		[x]
−127.5800	42.1900	11	MW-1	2830	500	1.78	3.75	211	1.83	*Dymond and Collier* [1988]; *Dymond et al.* [1992]	annual		[x]
−125.7700	42.0900	12	NS I	2829	500	4.98	4.40	88	3.88	*Dymond and Collier* [1988]; *Dymond et al.* [1992]	annual		
−123.0000	34.8330	13	M-S	4100	50	3.00	6.00	200	8.89	*Smith et al.* [1994]	26.02.90	24.10.91	[x]
−104.0000	8.8000	14	MANOP_ M	3150	100	1.50	3.85	257	2.84	*Dymond and Lyle* [1985]; *Dymond et al.* [1992]; *Emerson et al.* [1985]	12. 09. 80	23.10.81	[x]
−92.8000	6.5500	15	MANOP_ H	3565	20	1.40	2.56	183	1.77	*Dymond and Lyle* [1985]; *Dymond et al.* [1992]; *Emerson et al.* [1985]	20. 09. 80	17.10.81	[x]
−86.0000	0.0000	16	epac	2670	100	1.63	3.86	237	3.64	*Cobler and Dymond* [1980]; *Emerson and Bender* [1981]	annual		[x]
−85.5833	5.3667	17	PB	3860	300	4.31	4.07	94	3.47	*Wefer* [1989]	03.12.79	02.12.80	
−71.0000	39.0000	18	WD-1	2750	50	2.26	3.67	162	4.02	*Walsh et al.* [1991]	annual		
−71.0000	39.4167	19	WD-2	2300	50	2.81	3.55	126	3.56	*Walsh et al.* [1991]	annual		
−72.0000	38.0000	21	EB-3	2192	30	6.30	3.47	55	3.85	*Emerson and Bender* [1981]	annual		
−71.0000	38.0000	22	EB-4	2815	20	3.94	3.84	98	3.16	*Emerson and Bender* [1981]	annual		
−70.0000	38.0000	23	EB-5	2816	501	2.30	2.65	115	3.26	*Emerson and Bender* [1981]	annual		
−69.0000	38.0000	24	EB-6	3577	518	4.20	0.93	22	2.07	*Emerson and Bender* [1981]	annual		
−59.0000	38.0000	25	EB-7	3520	50	2.24	1.69	75	1.30	*Emerson and Bender* [1981]	annual		
−57.5167	−62.2500	26	KG1	1952	364	3.92	1.58	41	1.92	*Wefer* [1989]; *Lampitt and Antia* [1997]	1983–1986		interannual variations
−54.0000	13.0000	27	DE	5288	202	0.65	1.80	277	1.18	*Francois et al.* [1995]	01.11.77	01.02.78	
−28.0000	−7.5000	28	WA3	5570	539	0.36	1.72	478	0.90	*Lampitt and Antia* [1997]; *Ragueneau et al.* [2000]	annual		
−25.5670	−4.0000	29	WA1	5530	539	1.18	2.17	183	1.40	*Lampitt and Antia* [1997]	17.10.92	21.03.93	
−21.0000	18.6000	30	EUM-M	3100	100	1.93	1.45	75	4.79	*Bory et al.* [2001]	annual		
−20.7000	21.1000	31	CB2	4092	535	1.73	1.89	109	4.17	*Wefer and Fischer* [1993]; *Fischer et al.* [2000]	15.03.89	24.03.90	
−20.7000	21.2000	32	CB3	4094	537	2.05	1.88	92	4.17	*Fischer et al.* [2000]	29.04.90	08.04.91	
−20.7000	21.2000	33	CB4	4108	546	1.28	1.88	147	4.17	*Fischer et al.* [2000]	03.05.91	19.11.91	

Table 5. (continued)

Longitude[a]	Latitude[b]	Trap Number	Trap	wd, m	Trap Depth Above Bottom, m	$J_{POC\ Trap}$,[c] gC m^{-2} yr^{-1}	$J_{POC\alpha}$,[d] gC m^{-2} yr^{-1}	$J_{POC\alpha}/J_{POCTrap}$, %	J_{POC},[e] gC m^{-2} yr^{-1}	Editor	Start Date Trap	End Date Trap	Comment[f]
−20.7000	21.2000	34	CB-average	4108	539	1.69	1.88	116	4.17	*Fischer et al.* [2000]	15.03.89	19.11.91	interannual variations
−17.9543	29.7622	35	LPI	4327	527	0.58	2.08	358	0.89	*Lampitt and Antia* [1997]	06.01.97	01.09.97	interannual variations
−13.5200	48.9000	36	OMEX3-average	3260	40	2.13	2.15	101	1.92	*OMEX-I* [1997]	01.07.93	14.09.94	average of all OMEX-a data
−12.3400	49.5600	37.	OMEX2-average	1500	450	2.33	1.68	72	3.88	*OMEX-I* [1997]	01.07.93	14.09.94	average of all OMEX-a data
−11.1267	1.7917	38	GBN3-I	4481	560	2.20	2.03	92	2.85	*Wefer and Fischer* [1993]	01.03.89	25.02.90	
−9.9250	−2.1930	39	GBZ5	3920	538	2.37	1.26	114	3.09	*Lampitt and Antia* [1997]	4.4.90	30.3.91	
9.2000	−20.0000	40	WR-M	2263	555	3.78	3.97	121	6.32	*Fischer et al.* [2000]	04.03.88	17.12.91	interannual variations
61.5000	15.9833	41	MS-4	3974	496	3.25	4.29	132	4.52	*Honjo et al.* [1999]	11.11.94	24.12.95	
65.0000	10.0000	42	MS-5	4411	496	1.20	1.90	158	2.26	*Honjo et al.* [1999]	11.11.94	24.12.95	
135.1660	2.9967	43	K1	4413	512	5.15	2.53	49	1.73	*Kawahata* [2002]	27.04.92	25.11.00	
136.2766	4.1250	44	K2	4888	314	3.98	2.01	50	1.61	*Kawahata* [2002]	15.04.92	25.11.00	
154.8250	−17.7617	45	K12	2821	517	0.37	0.96	264	1.36	*Kawahata* [2002]	16.05.95	16.03.96	[x]
156.0000	−13.0000	46	K11	1832	517	0.99	1.61	163	1.61	*Kawahata* [2002]	01.04.96	16.11.00	
174.9450	37.4033	47	K7	5105	517	2.01	2.78	139	0.80	*Kawahata* [2002]	09.04.94	08.11.00	
175.0000	7.9266	48	K4	5260	517	0.51	0.97	190	0.71	*Kawahata* [2002]	13.04.93	17.07.00	
175.1500	0.0000	49	K3	4880	517	0.99	0.93	94	2.48	*Kawahata* [2002]	16.04.93	14.11.00	
177.7366	34.4217	50	K5	3365	517	2.81	2.30	82	1.28	*Kawahata* [2002]	01.06.94	15.12.00	
6.8000	78.9000	51	SP	1676	551	6.60	5.67	86	8.10	*Antia et al.* [2001]; *Hebbeln* [2000]	9.12.88	9.12.89	[x]
−7.7117	72.3817	52	OG72	2631	431	0.55	1.32	240	0.73	*Antia et al.* [2001]; *van Bodungen et al.* [1995]	25.2.91	25.2.92	[x]
0.4000	70.0000	53	NB-a	3269	269	3.56	1.86	52	0.23	*van Bodungen et al.* [1995]	1986	1989	[x]
0.4633	69.6867	54	NB-b	3292	292	2.76	1.99	72	0.19	*Thomsen* [1993]	6.8.91	3.7.92	[x]
1.0667	65.5167	55	NA-1	3058	428	0.59	2.49	422	0.62	*Wefer* [1989]	19.8.85	18.7.86	[x]
1.3667	78.8650	56	FS-1	2823	381	0.41	3.37	822	1.87	*Wefer* [1989]	10.8.84	30.7.85	[x]
10.0000	69.5000	57	LB (1)	3161	400	1.37	1.91	139	0.84	*Wefer* [1989]; *Francois et al.* [1995]	15.8.83	1.8.84	[x]
11.4660	75.8500	58	BI-1	2123	423	2.85	3.02	106	0.46	*Wefer* [1989]; *Francois et al.* [1995]	12.8.84	10.8.85	[x]
12.4867	75.1967	59	BI-2	2000	50	5.22	2.10	40	1.14	*Thomsen* [1993]	16.3.91	23.7.91	[x]
15.0000	74.0000	60	BS	1608	20	18.81	2.00	11	0.92	*Francois et al.* [1995]	18.5.89	10.8.89	[x]
−15.4500	29.1167	61	ESTOC	3600	523	0.84	2.63	313	1.35	*Neuer et al.* [1997]	25.11.1991	9.06.1994	[x]

[a]Longitude: west is negative.
[b]Latitude: south is negative.
[c]Particulate organic carbon fluxes collected by near bottom traps.
[d]Particulate organic carbon fluxes this study.
[e]Particulate organic carbon fluxes recalculated after *Antia et al.* [2001], for the Greenland-Norwegian-Iceland Sea recalculated after *Schlüter et al.* [2000].
[f]Here [x]: not included in regression analyses and not shown in Figures 10a and 10b.

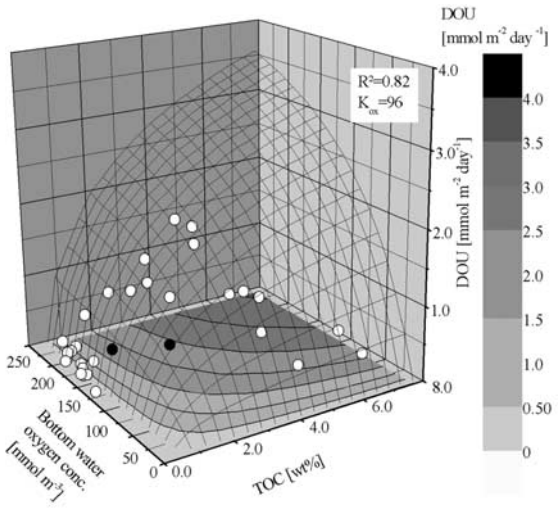

Figure 3a. Multiple regression analysis of the northeast Pacific Ocean and the continental margin of northwest America (NWAMCO). White circles indicate in situ DOU data used in the regression analyses; black circles indicate data not used in the regression analyses (BNTH-3-SBC [*Emerson et al.*, 1985] and Reimers_C-133_BC [*Reimers et al.*, 1992]) (>1000 m water depth). Grids represent fit functions.

deviations have to be discussed in more detail. For example, a relatively high $J_{POC\alpha}$ value was calculated at the confluence zone of the Malvinas and Brazil currents. We mainly traced this feature to the current pattern in this region, where intense flow velocities induce strong lateral transport processes [*Hensen et al.*, 2000; *Benthien and Müller*, 2000; *Frenz et al.*, 2003; *Hensen et al.*, 2003]. These caused particle winnowing (along the southwest slope off Argentine) and focusing (at the slope off southeast Brazil and in the Argentine Basin), and therefore resulted in decoupling of the vertical connection between primary production and sediment accumulation. Accordingly, particulate organic carbon fluxes, which are based on primary production and trap data, may be dubious under such conditions. Another difficulty underlying the problems with the simple assumption of a vertical link between the surface water and the sea floor is the variations in the intensity of mineralization processes. For example, $J_{POC\alpha}$ is lower in the deep eastern equatorial Atlantic than is predicted from primary production using a common power model. The reason could be that the oxygen-rich North Atlantic Deep Water favors the microbial degradation of organic matter as early as during the sedimentation process. A similar great influence on organic carbon mineralization accordingly affecting the low preservation potential was also proposed by *Curry and Lohmann* [1990] and recently confirmed by *Mollenhauer et al.* [2004] for the deep Guinea Basin.

[49] Upon comparing our results with *Antia et al.* [2001], we discovered that the most significant deviations can be observed with regard to the Pacific Ocean. However, owing to their great extensions, the deep-sea basins of the northern and southern Atlantic Ocean, the Pacific Ocean, and the Indian Ocean have the main impact on global J_{POC} budgeting. In total, they constitute 84% of the annual global amount of $J_{POC\alpha}$, which accumulates on 92% of the global sea floor (>1000 m wd, including equatorial areas). For example, the total budget of the eastern tropical Pacific Ocean is in the order of 14% of the globally integrated coastal budget (0.07 GtC yr^{-1}).

[50] However, the reliability of any lateral or nonlateral transport based distribution pattern of $J_{POC\alpha}$ is based on the data set being used. Single astonishing features in a global study have to be accounted for in the available database containing the TOC and oxygen flux measurements. It is noticeable that the astonishing high fluxes estimated, for example, south of the Hawaii Island result from individual TOC surface data in this region and should therefore be regarded critically as a possible artifact arising from unsuitable regression fits in this area. A summary of mean flux rates in the specific provinces is included in Table 4. These observations suggest looking at the trap data in more detail.

3.2.2. Trap-Based J_{POC} Versus $J_{POC\alpha}$

[51] Figure 10a contains direct comparisons between sediment trap data, J_{POC}, determined by *Antia et al.* [2001], and our own estimations of $J_{POC\alpha}$. Most of the values agree well with our estimations. The overall regression coefficient for measured particle fluxes and estimated $J_{POC\alpha}$ is $R = 0.69$ (Figures 10a and 10b). Considering the known biogeochemical and sedimentary processes that can affect the efficiency of trap collections, this correlation appears satisfactory at first glance. The estimations made by *Antia et al.* [2001] and our own estimations scatter around a regression curve with a slope of 1.1 and 0.96, respectively, which support our results indicating that both approaches produced a similar global budget. Nevertheless, there are still discrepancies at single locations.

[52] One of the most striking deviations of $J_{POC\alpha}$ and trap data arises in the western tropical Pacific Ocean (sites K1

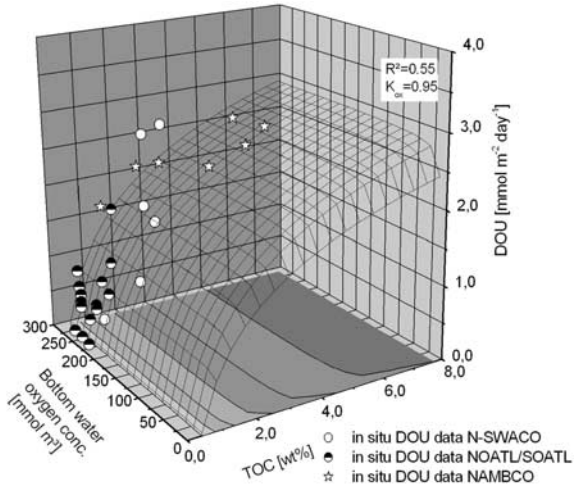

Figure 3b. Multiple regression analysis of the southeast Atlantic Ocean data representing the SWACO, NOATL/SOATL, and NAMBCO provinces.

Table 6. TOC_β Calculations Fixed and Not Fixed With Basin Data, Mean Sedimentation Rate (SR) Calculated for Each Province and Standard Deviation of SR (SD_{SR}), Calculated Burial Rate (β), and Range of TOC Data[a]

Province	$TOC^1{}_\beta$, wt%	$TOC^2{}_\beta$, wt%	SR, cm kyr^{-1}	SD_{SR}, cm kyr^{-1}	β, g m^{-2} yr^{-1}	TOC (Min), wt%	TOC (Max), wt%	TOC (Mean), wt%
WARAB/EARAB/	0.25	0.36	14.5 (4)/11.4 (5)	5.8/5.3	0.19–0.27/0.24–0.34	0.49/0.36	4.28/3.23	1.36/1.48
N-SWACO	0.11	0.77	9.6 (35)	18.5	0.07–0.48	0.35	3.01	1.21
NEAMCO	0.11	-	6.0 (2)	0	0.04	0.08	1.75	0.65
GUBRACO/BRAZCO	0.11		5.8 (7)/3.0 (5)	4.0/1.89		0.19/0.18	1.01/1.15	0.43/0.54
CANAR/WAFCO	-	-	-	-	-	0.32/0.09	1.04/1.94	0.62/0.64
RIOPLATA/ARGCO	0.09	0.31	23.1 (5)/3.9 (1)	18.4/–	0.14–0.47	0.26/0.12	3.36/0.77	0.94/0.38
EUR1	0.033	0.033	8.12 (1)	-	0.016	0.23	1.83	0.78
NOATL/SOATL	0.15	0.14	3.40 (113)/4.0 (95)	3.1/8.1	0.03/0.04	0.05/0.05	1.1/1.66	0.36/0.35
NAMBCO	0.17	-	17.3 (12)	29.7	0.19	0.30	4.86	1.87
GROE	0.21	0.45	4.6 (81)	10.8	0.06–0.12	0.08	1.57	0.72
LAPTEV SEA	-	0.61	19.0 (27)	13.1	0.76	0.48	1.53	0.97
TROPAC	-	0.30	1.6 (32)	0.91	0.03	0.12	4.74	1.22
NEPAC/NWAMCO[b]	-	0.25	1.16 (3)/–	1.4/–	0.02	0.06/0.3	1.74/5.49	0.44/1.56
CHICO/PERCO	-	0.14	4.92 (1)/6.5 (2)	–/3.5	0.003/0.004	0.3/1.63	3.97/7.58	1.45/3.82

[a]TOC_β is intersection point with the abscissae. $TOC^1\beta$ is mean refractory organic carbon based on regression fits fixed with basin data = lower limit. $TOC^2\beta$ is mean refractory organic carbon based on regression fits without basin data = upper limit. SR is mean sedimentation rate (SR) of each province, numbers in brackets: number of data points. SD_{SR} is standard deviation of SR. Here β is organic carbon burial rate, based on mean $TOC^{1,2}{}_\beta$, and mean sedimentation rates adopted from the literature. TOC is all calculations for water depth > 1000 m; min, max, and mean values of TOC are based on the projected grid (1° × 1°) after *Seiter et al*. [2003].

[b]No calculations of β for NWAMCO by missing intersection point (TOC_β).

and K2, Figure 10b (43 and 44)). While sediment traps detected a flux of 5.15 gC m^{-2} yr^{-1} (K1, see Table 5) and 3.98 gC m^{-2} yr^{-1} (K2, see Table 5), respectively, our results underestimated these values by a factor of ~0.5. The high J_{POC} by values based on trap data was mainly attributed to the large nutrient supply by estuarine upwelling and the deeper mixing of the upper water column [*Kawahata*, 2002]. Furthermore, there is a tremendous addition of terrestrial riverine discharges, and thus refractory organic carbon in this region [*Kawahata*, 1999; *Milliman et al.*, 1999; *Kawahata and Murayama*, 2000], which may favor a rapid downward transport associated with a reduced degradation within the water column. Since we transferred regression fits for the entire tropical Pacific Ocean to this area, we are not able to consider local circumstances and may have underestimated the organic carbon flux to the sea floor in this area. In addition, the approximation error adhering to the distribution pattern is within a factor of 0.5–2 (Figure 8). In comparison, trap data from stations K7 (see Table 5, Figure 10b (47) and K5 (see Table 5, Figure 10b (50)) almost coincide with our estimations.

[53] At sites LP1 and ESTOC (not shown in Figure 10b; see Table 5), both located close to the Canary Islands, $J_{POC\alpha}$ estimates and values from trap collections vary by a factor of ~3.4. Both sites are mainly characterized by an intense atmospheric dust input and lateral particle advection [*Neuer et al.*, 1997; *Wefer and Fischer*, 1993; *Freudenthal et al.*,

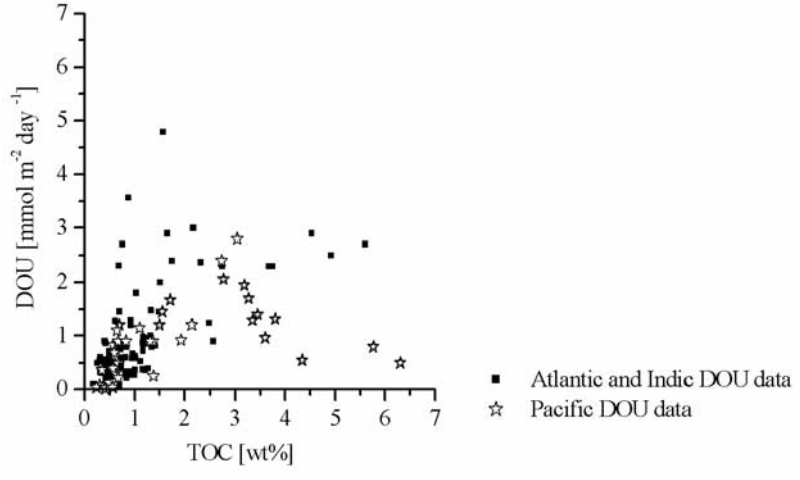

Figure 4. Summary of all DOU data versus TOC data used in this study. Solid squares represent DOU data pertaining to the Atlantic Ocean (including polar seas) and Indian Ocean. Stars represent data of the Pacific Ocean (>1000 m water depth, GROE > 550 m).

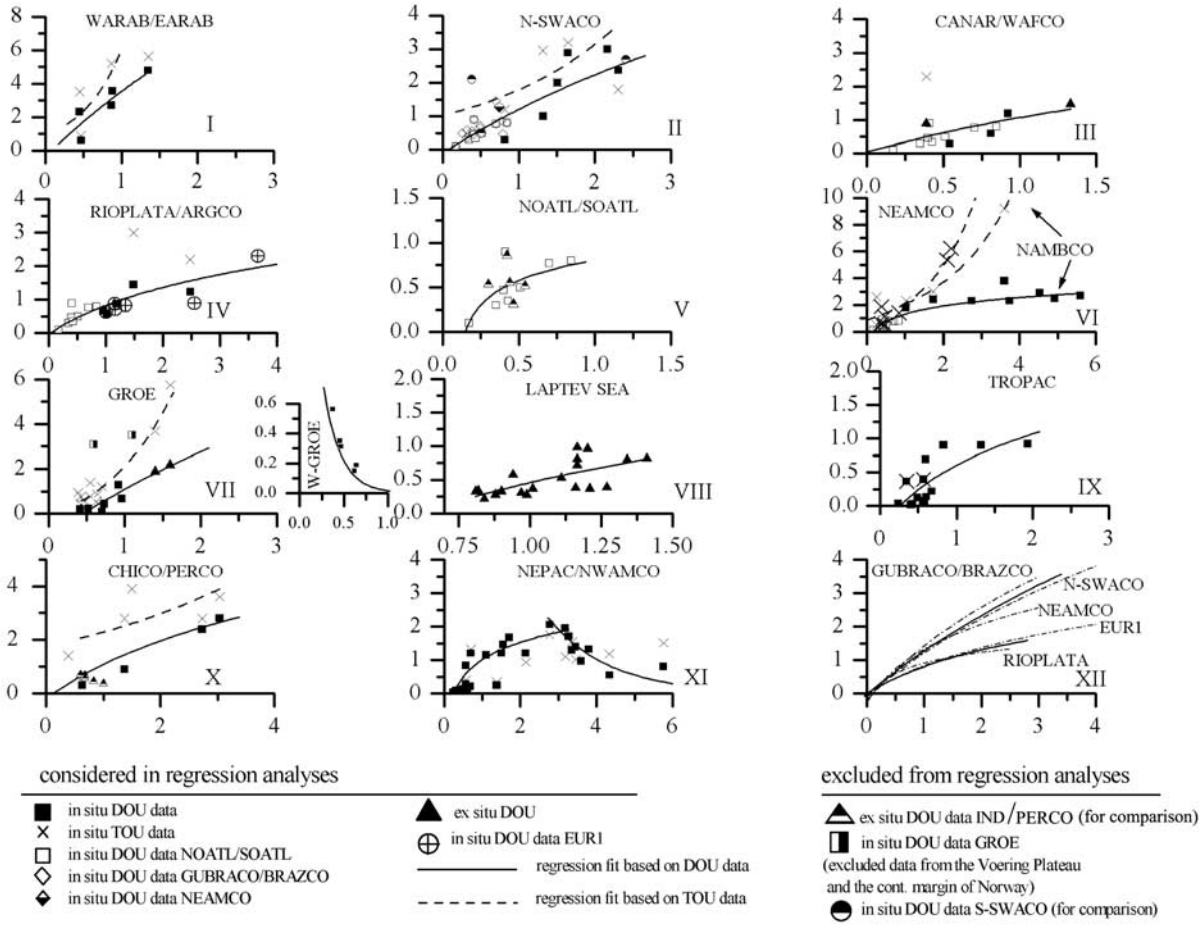

Figure 5a. Regression plots applying to specific regions. Ordinate: DOU (mmol m^{-2} d^{-1}) and TOU (mmol m^{-2} d^{-1}); abscissae: TOC (wt%). Solid squares: in situ DOU data; crosses: in situ TOU data. Regression in Figure 5a, fit XI, not included in 2-D-regression analyses (Figure 3a).

2001]. The latter is substantiated by time series data, which invariably show higher flux rates in the lower traps [*Lampitt and Antia*, 1997; *Neuer et al.*, 1997]. Therefore the discrepancy between trap data and the $J_{POC\alpha}$ seems to be attributable to an additional lateral input of organic carbon into the benthic nepheloid layer, not recorded by the traps [*Freudenthal et al.*, 2001]. A similar situation is known for the Arabian Sea (MS-4; MS-5, see Table 5, Figure 10b (41, 42)), where sea-floor mineralization rates and thus $J_{POC\alpha}$ exceed the input rates estimated from sediment traps [*Lee et al.*, 1998; *Pfannkuche and Lochte*, 2000].

[54] The trap data collections of trap stations EB-4 and EB-5 (see Table 3, Figure 10b (22, 23)), deployed above the organic carbon depot center at the continental margin of northeast America, are well represented by our estimations. Certainly, at EB-3, located nearshore, and EB-6 and EB-7, located far offshore (see Table 5), trap-based J_{POC} is consistently higher as inferred from oxic mineralization rates [*Biscaye et al.*, 1988]. This supports the idea of relatively rapid change of the benthic regimes to a higher portion of refractory organic matter toward the open ocean [*Walsh*, 1991; *Walsh et al.*, 1991; *Rowe et al.*, 1994]. However, at the nearshore site EB-3 (see Table 5), the underestimation of $J_{POC\alpha}$ could also be explained by our application of DOU instead of TOU [*Rowe et al.*, 1994] (Figure 5a (VI)).

[55] In general, the main decoupling process between estimates based on trap data and our estimates beyond a factor of 0.5–2 may consist in the lateral transport of particles. At sites additional to those discussed above, such transport processes can be assumed to exist. Therefore $J_{POC\alpha}$ indicates the lateral supply of POC near the sea floor at sites DE, WA3, and WA1 offshore Guyana and Brazil, and P1 in the northeast Pacific Ocean (see Table 5 and Figure 10b in the above-mentioned order (27, 28, 29, 1)).

3.3. Effect When Using TOU Instead of DOU

[56] All calculations discussed so far are based on DOU measurements. However, as mentioned before, the total oxygen uptake (TOU) occurring especially along continental margins can be several times higher, due to bioirrigation of macrobenthic organisms [*Glud et al.*, 1994; *Archer and Devol*, 1992]. In the following, we want to question the effect of this neglect in the calculation of $J_{POC\alpha}$. The mean values of $J_{POC\alpha}$ applying to the specific provinces

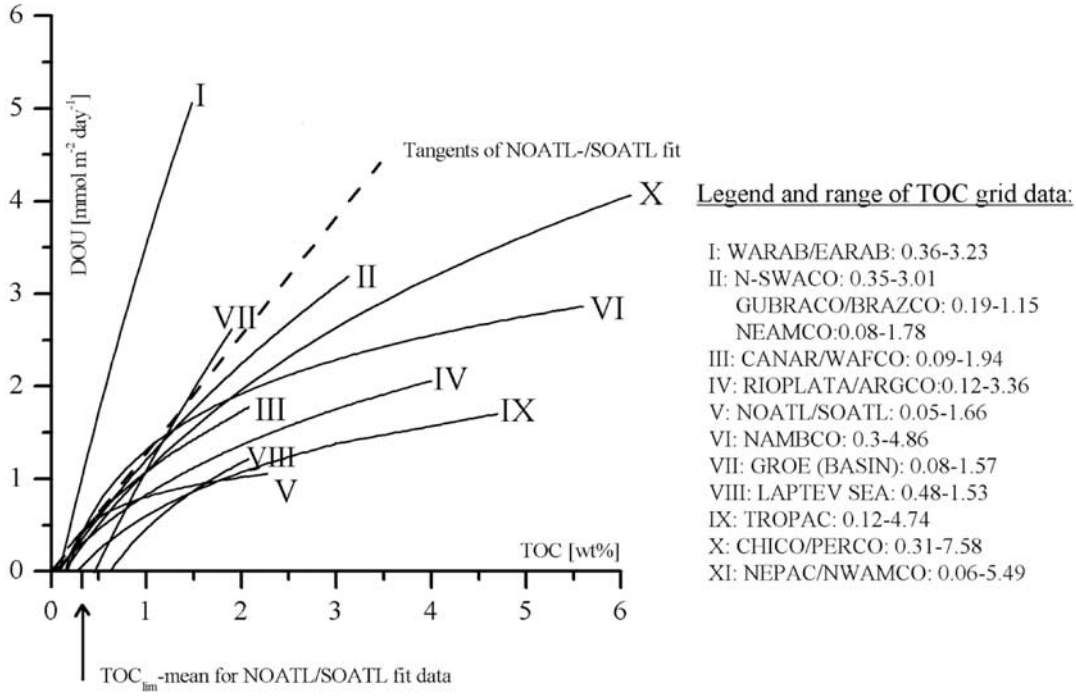

Figure 5b. Comparison of all regression fits valid in the range of TOC contents (grid based). Numbers represent the respective regression types shown in Table 3. Black arrow indicates TOC_{lim} as based on NOATL/SOATL fit data. The regression plot of NEPAC/NWAMCO (fit XI) is not shown.

are displayed in Figure 11. As to regions in which sufficient in situ TOU data were available, we also estimated the corresponding particulate organic carbon flux to the sea floor ($J_{POC\gamma}$). Except for using equation (5), the processing is the same as for $J_{POC\alpha}$. Of course, $J_{POC\gamma}$ generally exceeds $J_{POC\alpha}$ at the continental margin provinces (Figure 11). The greatest difference can be detected in the upwelling area off Namibia (NAMBCO), where a mean TOU of 5.1 mmol m^{-2} d^{-1} corresponds to an average rain rate of 17.2 gC m^{-2} yr^{-1}. Compared with the DOU- based $J_{POC\alpha}$ rate of 5.6 gC m^{-2} yr^{-1}, a TOU:DOU ratio of 3.1 can be derived. For comparable regions, SWACO, adjacent to the north, and the high productive areas off Chile (CHICO), and the Arabian Sea, this ratio is 1.7, which would agree with the lower TOC contents of these sediments. However, it does not astonish that zones with other benthic and sedimentary conditions do not fit into this supposedly simple trend.

[57] TOU:DOU ratios of 2.6 and 1.6 seem to be characteristic of the northeast American continental margin (NEAMCO) and the Greenland-Norwegian-Iceland Sea (GROE), respectively, where the mean TOC contents are comparatively low (0.65 and 0.72 wt%). The reason may be the same as discussed above (section 3.1). However, due to the reduced activity of benthic organisms, no significant differences between $J_{POC\alpha}$ and $J_{POC\gamma}$ can be observed within the deep-sea basins of the Atlantic Ocean and the northeast Pacific Ocean (TOU:DOU $\approx$ 1). As these constitute ~80% of the global sea floor, the extrapolation of our $J_{POC\gamma}$ estimates to the entire ocean yields a minimum organic carbon rain rate of approximately 0.60 GtC yr^{-1}. The factor of 1.2 arising when TOU instead of DOU is used to calculate the global benthic carbon flux only corresponds very well to results allocated to the Atlantic Ocean [*Wenzhöfer and Glud*, 2002].

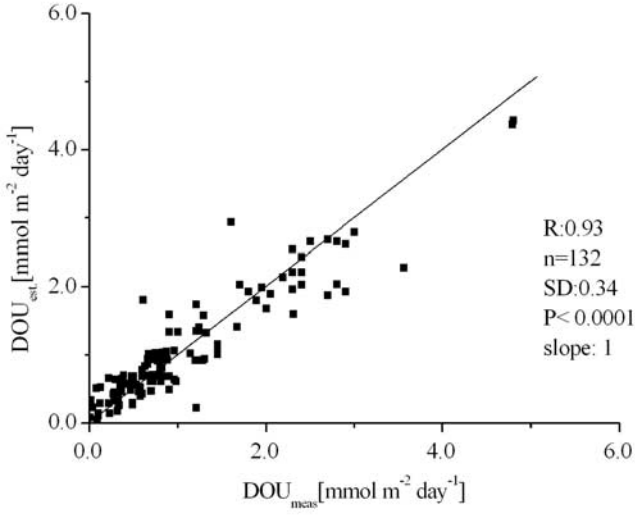

Figure 6. Estimation accuracy of all regression fits within 83.5°N–85°S, displayed as estimated DOU (DOU_{est}) versus measured DOU (DOU_{meas}). Bisecting line shows regression fit.

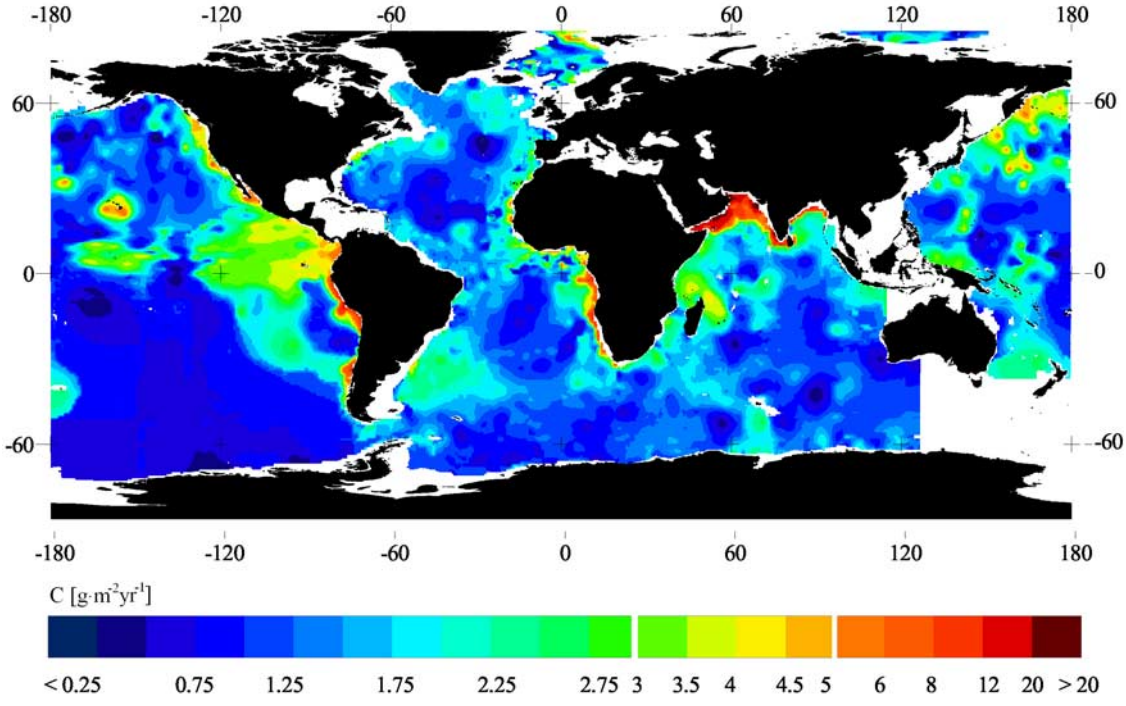

Figure 7. Global distribution pattern of the calculated minimum flux of particulate organic carbon to the sea floor ($J_{POC\alpha}$; 1° × 1°; > 1000 m wd) based on global estimates of in situ diffusive oxygen uptake (DOU). $J_{POC} = 0.77 \times DOU$.

3.4. Estimation of Mean Burial Rates

[58] As described above, the mean content of refractory organic carbon (TOC_β) in single provinces was derived from the relation between DOU and TOC (Figure 5a (I–XI)). Thus, based on the assumption that no further oxygen uptake occurs, we interpret the intersection point of the abscissa as an indicator for TOC_β expressed in wt%. The mean burial rates were calculated accordingly, by multiplying TOC_β with the mean sedimentation rates (SR) and the dry bulk density (DBD) in the appropriate provinces, (section 2.2; equation (7), Table 6).

[59] In order to calculate the global budget of buried organic matter, we calculated a range of the burial rate, using the lower and upper limits of SR and TOC_β, respectively. An extrapolation of the global ocean budget was performed, observing the relative proportion of the specific province areas.

[60] The lower limit is the TOC_β value derived from the regression fits shown in Figures 5a (I–XI) and 5b) and summarized in Table 6. Upon calculating these lower limits, we considered the adjacent basin data if a province bordered on the deep-sea basin, in order to characterize the transition between the continental margin and basin areas. The upper TOC_β limit characterizes the refractory organic carbon content within a continental margin province, calculated during regression analyses without integration of the basin data (section 2.2). The mean SR, the TOC_β range, and the standard deviation of the SR (SD) for appropriate benthic provinces are summarized in Table 6. As a result, the burial

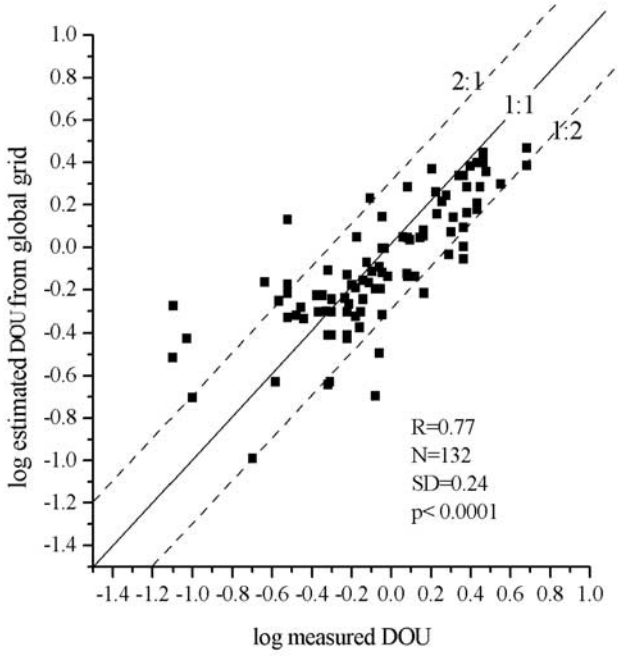

Figure 8. Comparison of oxygen flux measurements and estimated flux values (DOU) after applying regression fits to the regular TOC grid. Estimated values were queried from the global grid (DOU) before calculating the $J_{POC} = 0.77 \times DOU$ (see Figure 7).

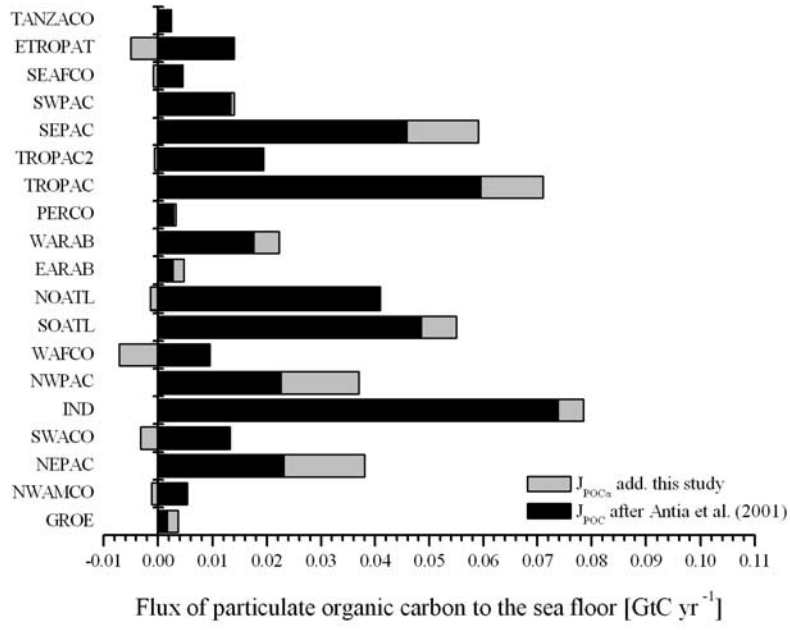

Figure 9. Comparison of recalculated flux of particulate organic carbon to the sea floor (J_{POC}) as estimated by *Antia et al.* [2001] (Gt C yr^{-1}) (black bars) and calculated $J_{POC\alpha}$ (this study). The gray fraction of the horizontal bar chart shows the additional or reduced calculated portion of $J_{POC\alpha}$ resulting from this study. Provinces with less than 0.002 GtC yr^{-1} budget in each province are not shown; see Table 3 (NEAMCO, GUI, CHICO, GUBRACO, ARGCO, BRAZCO, CANAR, EUR1, EUR2, RIOPLATA, NAMBCO, EICO, ANT, SOMALICO).

rates were found to be low in the basin areas of the northern Pacific Ocean and the southern and northern Atlantic Ocean, and to increase towards the continental margins. An average burial rate of 0.03–0.04 gC m^{-2} yr^{-1} has been estimated for the eastern tropical Pacific Ocean and the northern and southern Atlantic Ocean. This value is slightly lower (0.02 gC m^{-2} yr^{-1}) as far as the northeast Pacific Ocean is concerned. The highest rates were identified in the Arabian Sea and along the continental margin of southwest Africa (SWACO), amounting to 0.19–0.34 gC m^{-2} yr^{-1} and 0.07–0.48 gC m^{-2} yr^{-1}, respectively. However, all these values were based on mean TOC_{β} and mean SR values in the corresponding provinces. Thus, regional and seasonal variabilities were not accounted for and the deviations from the mean values applying to specific areas might have a tremendous effect in some exceptional cases. Overestimation of mean burial rates could be due to disregarding the anaerobic mineralization in sediments and the nondiffusive, fauna-mediated oxygen uptake in predominantly coastal sediments. Areal integration resulted in a global organic carbon burial rate ranging approximately from 0.002 to 0.12 GtC yr^{-1}. Hence ~0.01–0.4% of the primary production should be stored in the sediments of the predominantly oligotrophic open-ocean areas and withdrawn from the global cycle for a longer period of time. In comparison, the global $J_{POC\alpha}$ budget accounted for ~1.6% of the surface primary production [*Antoine et al.*, 1996]. If we include the organic carbon flux through the 1000-m-depth horizon as previously published by *Jahnke* [1996] (0.86 GtC yr^{-1}), ~40% of this amount is degraded in the deeper water column. With other estimates of the flux leaving the surface mixed layer ((2.3 GtC yr^{-1}) [*Christensen*, 2000] and (2.47 GtC yr^{-1}) [*Antia et al.*, 2001]), this value would increase twofold up to ~80%.

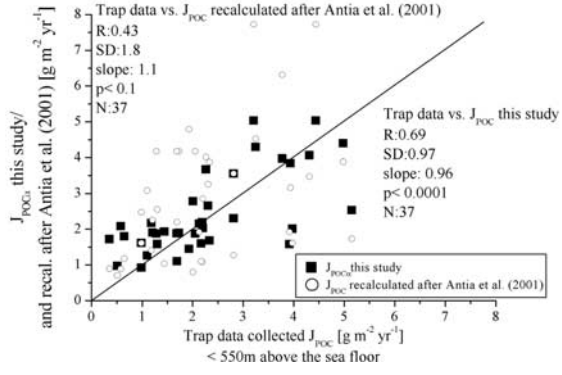

Figure 10a. Regression plot of $J_{POC\alpha}$ (this study) versus J_{POC} derived data from samples obtained by traps (maximum ~550 m above the sea floor) marked as solid black circles and J_{POC} recalculations as estimated by *Antia et al.* [2001] versus J_{POC} derived data by traps (marked as open circles). Trap sites excluded from regression analyses: MANOP_H, MANOP_S, MANOP_M; MSZ-11; epac; K12; P1; MW-1, M-S; EB-3, 6, 7 and all data from the Greenland-Norwegian-Iceland Sea (see Table 5). Solid line is bisecting line.

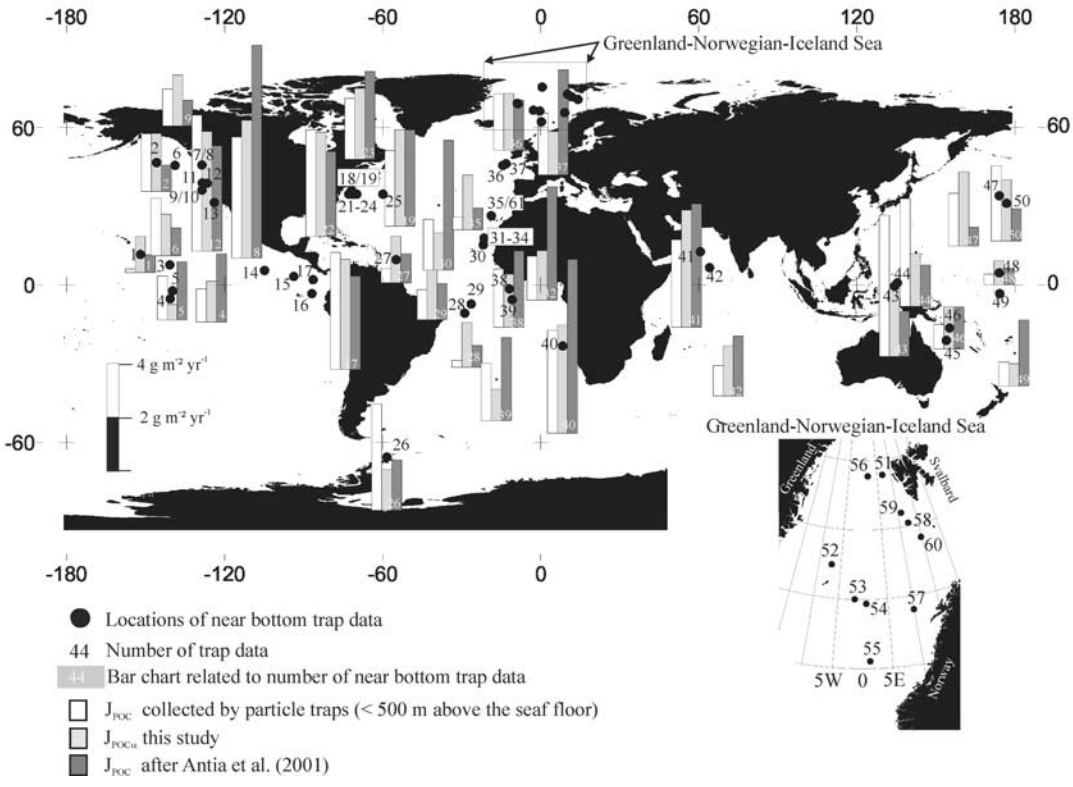

Figure 10b. Bar charts for comparisons of sediment trap data observations with $J_{POC\alpha}$ of this study and flux recalculations after *Antia et al.* [2001]. All trap data are numbered and summarized in Table 5.

Nevertheless, detailed re-evaluations concerning the mineralization in the deeper water column are not addressed in this paper. However, undoubtedly, as follows from the relationship between $J_{POC\alpha}$ and TOC_{β}, the majority of the particulate organic matter reaching the sea floor is remineralized in short periods of time.

4. Conclusions

[61] Understanding the temporal progression and balance of the global carbon cycles has been a focus of former and recent research studies during the last few decades. The biological organic carbon pump and the prediction of present-day ocean carbon sinks and sources are of increasing interest. Since both the deposition of organic carbon on the sea floor and the deep-sea organic carbon fluxes are representative of potential carbon sinks, their prediction is a basic necessity. In this context, the immense importance of dissolved free oxygen in the microbial decomposition of organic matter is well known, but the number of reliable and comparable measurements is low and often restricted to certain regions. Additionally, several locally restricted benthic processes affect the organic carbon particle rain and accumulation rate on the sea floor, which results in a decoupling of remote-sensed chlorophyll distribution patterns and productivity flux/water-depth relationships. The great advantage and improvement of our method presented here is the view from the benthic side, accounting for different sedimentary and geochemical regimes in 11 benthic provinces. The estimation is mainly based on the relation between the diffusive oxygen flux across the sediment-water interface (DOU) and the content of total organic carbon in the surface sediments (TOC). The incomplete database of oxygen consumption rates can be gripped by using the highly disposable sedimentary proxy parameter, i.e., the total organic carbon content (TOC) in surface sediments. DOU as the most readily available benthic oxygen flux parameter is regarded as equivalent to the organic carbon mineralization and the minimum of organic carbon that settles on the sea floor ($J_{POC\alpha}$). The province-specific results obtained from 11 regression fits between single measurements and the control parameter TOC were extrapolated on the global scale. Differences in the availability and the quality of organic matter, or in the mechanisms of transport through the water column, are reflected by individual regression fits in the provinces. We avoided the use of sedimentation rates, which are relatively limited by number in the current database and mostly susceptible to errors caused by uncertainties in age models. Thus, regional lateral supply or winnowing of sedimentary organic carbon can affect the vertical link between surface water and sea floor, and could be taken into account by province-specific regression fit between TOC and DOU. This is clearly reflected by the deviations of $J_{POC\alpha}$ estimations of this study, estimations obtained from common power models [*Antia et al.*, 2001], and bottom near-trap data.

[62] Globally, however, our estimations stand in good accordance with former investigations [*Jahnke*, 1996; *Antia*

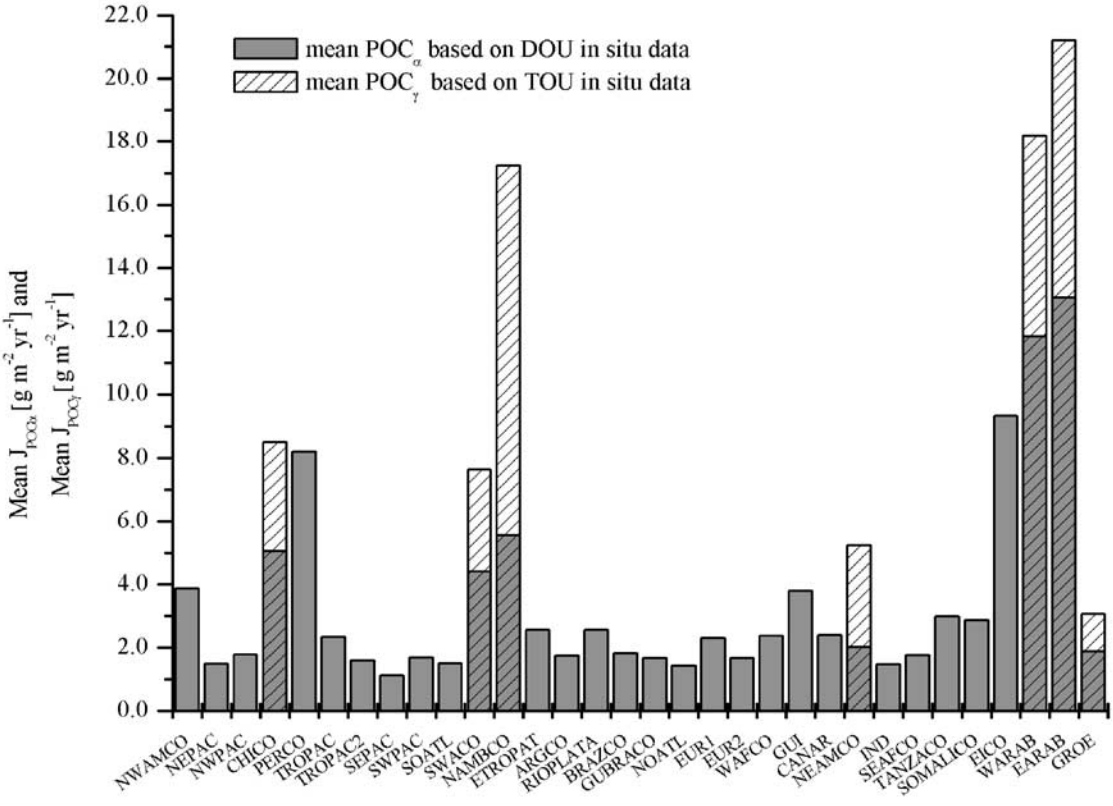

Figure 11. Mean $J_{POC\alpha}$ (queried from the grid, Figure 7) to the sea floor (gray bars), and mean $J_{POC\gamma}$ (white bars, equation (5)). LAPTEV SEA is not shown.

et al., 2001]. The global $J_{POC\alpha}$ budget was estimated to be at ~0.5 GtC yr^{-1} (>1000 m wd), whereas approximately 0.002–0.12 GtC yr^{-1} were buried in the sediments (0.01–0.4% of surface primary production). The rough extrapolation of the total organic carbon flux ($J_{POC\gamma}$) to the entire ocean yielded a minimum organic carbon rain rate of approximately 0.60 GtC yr^{-1}, which is a factor of approximately 1.2 higher than expected when using TOU instead of DOU. The new approach of transferring regional benthic provinces based on TOC offers new opportunities in estimations of biogeochemical budgets and sinks of organic carbon, respectively. Future studies should include other sedimentary parameters such as opal, calcite, and terrigenous lithogenic components, next to more sophisticated age models, to considerably improve province-specific regression analyses and related estimations.

[63] **Acknowledgments.** We would like to thank H. Hecht, K. Pfeifer, N. Riedinger and A. Schäfer for valuable and critical comments in the process of improving the manuscript. We also gratefully appreciate the support from M. Diepenbroek, L. Gerullis and R. Sieger (*Pangaea* – Network for Geological and Environmental Data). Many thanks also to all the unnamed colleagues who did not hesitate to provide their data. We appreciated the very helpful and detailed comments of the reviewers, which did improve the original version of this manuscript. Most of the critical aspects, which were pointed out could be addressed and are now considered in the manuscript. This study was funded by the Deutsche Forschungsgemeinschaft by a special project (ZA 199) and the DFG-Research Center Ocean Margins, Contribution No. RCOM0136.

References

Anderson, L. A., and J. L. Sarmiento (1994), Redfield ratios of remineralization determined by nutrient data analysis, *Global Biogeochem. Cycles*, *8*, 65–80.

Antia, A. N., et al. (2001), Basin-wide particulate carbon flux in the Atlantic Ocean: Regional export patterns and potential for atmospheric CO_2 sequestration, *Global Biogeochem. Cycles*, *15*, 845–862.

Antoine, D., J.-M. André, and A. Morel (1996), Oceanic primary production: 2. Estimation at global scale from satellite (coastal zone color scanner) chlorophyll, *Global Biogeochem. Cycles*, *10*, 57–69.

Archer, D. E. (1996), An atlas of the distribution of calcium carbonate in sediments of the deep sea, *Global Biogeochem. Cycles*, *10*, 159–174.

Archer, D., and A. Devol (1992), Benthic oxygen fluxes on the Washington shelf and slope: A comparison of in situ microelectrode and chamber flux measurements, *Limnol. Oceanogr.*, *37*, 614–629.

Armstrong, R. A., C. Lee, J. I. Hedges, S. Honjo, and S. G. Wakeham (2002), A new mechanistic model for organic fluxes in the ocean based on the quantitative association of POC with ballast minerals, *Deep Sea Res., Part II*, *49*, 219–236.

Arthur, M. A., W. E. Dean, and K. Laarkamp (1998), Organic carbon accumulation and preservation in surface sediments on the Peru margin, *Chem. Geol.*, *152*, 273–286.

Behrenfeld, M. J., and P. G. Falkowski (1997a), A consumer's guide to phytoplankton primary productivity models, *Limnol. Oceanogr.*, *42*, 1479–1491.

Behrenfeld, M. J., and P. G. Falkowski (1997b), Photosynthetic rates derived from satellite-based chlorophyll concentration, *Limnol. Oceanogr.*, *42*, 1–20.

Benthien, A., and P. J. Müller (2000), Anomalously low alkenone temperatures caused by lateral particle and sediment transport in the Malvinas Current region, western Argentine Basin, *Deep Sea Res., Part I*, *47*(12), 2369–2393.

Berelson, W. (2002), Particle settling rates increase with depth in the ocean, *Deep Sea Res., Part II*, *49*, 237–251.

Berger, W. H., V. S. Smetacek, and G. Wefer (1989), Ocean productivity and paleoproductivity—An overview, in *Productivity of the Ocean: Present and Past*, edited by W. H. Berger et al., pp. 1–34, John Wiley, Hoboken, N. J.

Betts, J. N., and H. D. Holland (1991), The oxygen content of ocean bottom waters, the burial efficiency of organic carbon, and the regulation of atmospheric oxygen, *Palaeogeogr. Palaeoclimatol. Palaeoecol.*, *97*, 5–18.

Betzer, P. R., W. J. Showers, E. A. Laws, C. D. Winn, G. R. DiTullio, and P. M. Kroopnick (1984), Primary productivity and particle fluxes on a transect of the equator at 153°W in the Pacific Ocean, *Deep Sea Res.*, *31*, 1–11.

Biscaye, P. E., R. Anderson, and B. L. Deck (1988), An indication of lateral input of biogenic detritus, *Deep Sea Res., Part II*, *41*, 657–668.

Bory, A., et al. (2001), Downward particle fluxes within different productivity regimes off the Mauretanien upwelling zone (EUMELI program), *Deep Sea Res., Part I*, *48*, 2251–2282.

Boudreau, B. P. (1997), *Diagenetic Models and Their Implication: Modelling Transport and Reactions in Aquatic Sediments*, pp. 142–159, Springer-Verlag, New York.

Bremner, J. M. (1983), Biogenic sediments on the South West African (Namibian) continental margin, in *Coastal Upwelling: Its Sedimentary Record*, edited by A. Suess and J. Thiede, pp. 73–103, Plenum, New York.

Bremner, J. M., and P. C. Willis (1993), Mineralogy and geochemistry of the clay fraction of sediments from the Namibian continental margin and the adjacent hinterland, *Mar. Geol.*, *115*, 85–116.

Cai, W.-J., and C. E Reimers (1995), Benthic oxygen flux, bottom water oxygen concentration and core top organic carbon content in the deep northeast Pacific Ocean, *Deep Sea Res., Part I*, *42*(10), 1681–1699.

Calvert, S. E., and T. F. Pedersen (1992), Organic carbon accumulation and preservation in marine sediments: How important is anoxia?, in *Organic Matter: Productivity, Accumulation, and Preservation in Recent and Ancient Sediments*, edited by J. K. Whelan and J. W. Farrington, Columbia Univ. Press, New York.

Calvert, S. E., and N. B. Price (1983), Geochemistry of Namibian shelf sediments, in *Coastal Upwelling: Its Sedimentary Record*, edited by J. Thiede and E. Suess, pp. 337–375, Plenum, New York.

Castro, C. G., F. P. Chavez, and C. A. Collins (2001), Role of the California Undercurrent in the export of denitrified waters from the eastern tropical North Pacific, *Global Biogeochem. Cycles*, *15*, 819–830.

Christensen, J. P. (2000), A relationship between deep-sea benthic oxygen demand and oceanic primary productivity, *Oceanol. Acta*, *23*, 65–82.

Cobler, R., and J. Dymond (1980), Sediment trap experiment on the Galapagos, equatorial Pacific, *Science*, *209*, 801–803.

Curry, W. B., and G. P. Lohmann (1990), Reconstructing past particle fluxes in the tropical Atlantic Ocean, *Paleoceanography*, *5*, 487–505.

Dowdeswell, J. A., A. Elverhoi, and R. Spielhagen (1998), Glaciomarine sedimentary processes and facies on the polar North Atlantic Margins, *Quat. Sci. Rev.*, *17*, 243–272.

Duineveld, G. C. A., P. A. W. J. De Wilde, E. M. Berghuis, A. Kok, T. Tahey, and J. Kromkamp (1997), Benthic respiration and standing stock on two contrasting continental margins in the western Indian Ocean: The Yemen-Somali upwelling region and the margin off Kenya, *Deep Sea Res., Part II*, *44*, 1293–1317.

Dymond, J., and R. Collier (1988), Biogenic particle fluxes in the equatorial Pacific: Evidence for both high and low productivity during the 1982–1983 El Niño, *Global Biogeochem. Cycles*, *2*, 129–137.

Dymond, J., and M. Lyle (1985), Flux comparisons between sediments and sediment traps in the eastern tropical Pacific: Implications for atmospheric CO_2 variations during the Pleistocene, *Limnol. Oceanogr.*, *30*, 699–712.

Dymond, J., and M. Lyle (1994), Particle fluxes in the ocean and implications for sources and preservation of ocean sediments, in *Material Fluxes on the Surface of the Earth*, pp. 125–142, Natl. Acad., Washington, D. C.

Dymond, J., E. Suess, and M. Lyle (1992), Barium in deep-sea sediment: A geochemical proxy for paleoproductivity, *Paleoceanography*, *7*, 163–181.

Eicken, H. (2003), The role of arctic sea ice in transporting and cycling terrestrial organic matter, in *The Organic Carbon Cycle in the Arctic Ocean*, edited by R. Stein and R. W. MacDonald, pp. 45–53, Springer-Verlag, New York.

Emerson, S., and M. Bender (1981), Carbon fluxes at the sediment-water interface of the deep-sea: Calcium carbonate preservation, *J. Mar. Res.*, *39*, 139–162.

Emerson, S., K. Fischer, C. Reimers, and D. Heggie (1985), Organic carbon dynamics and preservation in deep-sea sediments, *Deep Sea Res.*, *32*, 1–21.

Epping, E. H. G., C. van der Zee, K. Soetaert, and W. Helder (2002), On the oxidation and burial of organic carbon in sediments of the Iberian Margin and Nazare Canyon (NE Atlantic), *Prog. Oceanogr.*, *52*, 399–431.

Ewing, M., W. J. Ludwig, and J. I. Ewing (1964), Sediment distribution in the oceans: The Argentine Basin, *J. Geophys. Res.*, *69*, 2003–2033.

Fischer, G., G. Ratmeyer, and G. Wefer (2000), Organic carbon fluxes in the Atlantic and Southern Ocean: Relationship to primary production compiled from satellite radiometer data, *Deep Sea Res., Part II*, *47*, 1961–1997.

Francois, R., S. Honjo, S. J. Manganini, and G. E. Ravizza (1995), Biogenic barium fluxes to the deep sea: Implications for paleoproductivity reconstruction, *Global Biogeochem. Cycles*, *9*, 289–303.

Frenz, M., R. Heinrich, R. Höppner, J. B. Stuut, and T. Wagner (2003), Surface sediment bulk geochemistry and grain size composition related to oceanic circulation along the South American continental margin in the Southwest Atlantic, in *The South Atlantic in the Late Quaternary: Reconstruction of Material Budget in Current Systems*, edited by G. Wefer et al., pp. 343–373, Springer-Verlag, New York.

Freudenthal, T., S. Neuer, H. Meggers, R. Davenport, and G. Wefer (2001), Influence of lateral particle advection and organic matter degradation on sediment accumulation and stable nitrogen isotope ratios along a productivity gradient in the Canary Island region, *Mar. Geol.*, *177*, 93–109.

Freudenthal, T., H. Meggers, J. Henderiks, H. Kuhlmann, A. Moreno, and G. Wefer (2002), Upwelling intensity and filament activity off Morocco during the last 250,000 years, *Deep Sea Res., Part II*, *49*, 3655–3674.

Froelich, P. N., G. P. Klinkhammer, M. L. Bender, N. A. Luedtke, G. R. Heath, D. Cullen, P. Dauphin, D. Hammond, B. Hartman, and V. Maynard (1979), Early oxidation of organic matter in pelagic sediments of the eastern equatorial Atlantic: Suboxic diagenesis, *Geochim. Cosmochim. Acta*, *43*, 1075–1088.

Garzoli, S. R. (1993), Geostrophic velocity and transport variability in the Brazil-Malvinas Confluence, *Deep Sea Res., Part I*, *40*, 1379–1403.

Giraudeau, J., P. A. Meyers, and B. A. Christensen (2002), Accumulation of organic and inorganic carbon in Pliocene-Pleistocene sediments along the southwestern African margin, *Mar. Geol.*, *180*, 49–69.

Glud, R. N., J. K. Gundersen, N. P. Revsbech, and B. B. Jorgensen (1994), Effects on the benthic diffusive boundary layer imposed by microelectrodes, *Limnol. Oceanogr.*, *39*, 462–467.

Glud, R. N., J. K. Gundersen, and O. Holby (1999), Benthic in situ respiration in the upwelling area off central Chile, *Mar. Ecol. Prog. Ser.*, *186*, 9–18.

Goni, G. J. (2001), Investigation of the Brazil Current front variability from altimeter data, *J. Geophys. Res.*, *106*, 117–131.

Grutters, M., W. van Raaphorst, and W. Helder (2001), Total hydrolysable amino acid mineralisation in sediments across the northeastern Atlantic continental slope (Goban Spur), *Deep Sea Res., Part I*, *48*, 811–832.

Haake, B., V. Ittekkot, T. Rixen, V. Ramaswamy, R. R. Nair, and W. B. Curry (1993), Seasonality and interannual variability of particle fluxes to the deep Arabian Sea, *Deep Sea Res., Part I*, *40*, 1323–1344.

Haese, R. R., K. Wallmann, A. Dahmke, U. Kretzmann, P. J. Müller, and H. D. Schulz (1997), Iron species determination to investigate early diagenetic reactivity in marine sediments, *Geochim. Cosmochim. Acta*, *61*, 63–72.

Hartnett, H. E., R. G. Keil, J. I. Hedges, and A. H. Devol (1998), Influence of oxygen exposure time on organic carbon preservation in continental margin sediments, *Nature*, *391*, 572–574.

Hebbeln, D. (2000), Flux of ice-rafted detritus from sea ice in the Fram Strait, *Deep Sea Res., Part I*, *47*, 1773–1790.

Hebbeln, D., M. Marchant, T. Freudenthal, and G. Wefer (2000), Surface sediment distribution along the Chilean continental slope related to upwelling and productivity, *Mar. Geol.*, *164*, 119–137.

Hedges, J. I. (1992), Global biogeochemical cycles: Progress and problems, *Mar. Chem.*, *39*, 67–93.

Hedges, J. I., and R. G. Keil (1995), Sedimentary organic matter preservation: an assessment and speculative synthesis, *Mar. Chem.*, *49*, 81–115.

Hensen, C., M. Zabel, and H. D. Schulz (2000), A comparison of benthic nutrient fluxes from deep-sea sediments of Namibia and Argentina, *Deep Sea Res., Part II*, *47*, 2029–2050.

Hensen, C., M. Zabel, K. Pfeifer, T. Schwenk, K. Kasten, N. Riedinger, H. D. Schulz, and A. Boetius (2003), Control of sulfate pore-water profiles by sedimentary events and the significance of anaerobic oxidation of methane for the burial of sulfur in marine sediments, *Geochim. Cosmochim. Acta*, *67*, 2631–2647.

Holtvoeth, J., T. Wagner, B. Horsfield, C. J. Schubert, and U. Wand (2001), Late-Quaternary supply of terrigenous organic matter to the Congo deep-sea fan (ODP site 1075): Implications for equatorial African paleoclimate, *Geo Mar. Lett.*, *21*, 23–33.

Honjo, S., S. Manganini, and J. Cole (1982), Sedimentation of biogenic matter in the deep ocean, *Deep Sea Res.*, *29*, 609–625.
Honjo, S., J. Dymond, R. Collier, and S. J. Manganini (1995), Export production of particles to the interior of the equatorial Pacific Ocean during the 1992 EqPac experiment, *Deep Sea Res., Part II*, *47*, 831–870.
Honjo, S., J. Dymond, W. Prell, and V. Ittekkot (1999), Monsoon-controlled export fluxes to the interior of the Arabian Sea, *Deep Sea Res., Part II*, *46*, 1859–1902.
Hulth, S., P. O. J. Hall, T. H. Blackburn, and A. Landén (1996), Arctic sediments (Svalbard): Pore water and solid phase distributions of C, N, P and Si, *Polar Biol.*, *16*, 447–462.
Ittekkot, V. (1988), Global trends in the nature of organic matter in river suspensions, *Nature*, *332*, 436–438.
Ittekkot, V. (1993), The abiotically driven biological pump in the ocean and short-term fluctuations in atmospheric CO_2 contents, *Global Planet. Change*, *8*, 17–25.
Jahnke, R. A. (1996), The global ocean flux of particulate organic carbon: Areal distribution and magnitude, *Global Biogeochem. Cycles*, *10*, 71–88.
Jahnke, R. A., and G. A. Jackson (1987), Role of sea floor organisms in oxygen consumption in the deep North Pacific Ocean, *Nature*, *329*, 621–623.
Jahnke, R. A., and G. A. Jackson (1992), The spatial distribution of sea floor oxygen consumption in the Atlantic and Pacific Oceans, in *Deep-Sea Food Chains and the Global Carbon Cycle*, edited by G. T. Rowe and V. Pariente, pp. 295–307, Kluwer Acad., Norwell, Mass.
Jahnke, R. A., C. E. Reimers, and D. B. Craven (1990), Intensification of recycling of organic matter at the sea floor near ocean margins, *Nature*, *348*, 50–54.
Kawahata, H. (1999), Fluctuations in the ocean environment within the western Pacific warm pool during late Pleistocene, *Paleoceanography*, *14*, 639–652.
Kawahata, H. (2002), Suspended and settling particles in the Pacific, *Deep Sea Res., Part II*, *49*, 5647–5664.
Kawahata, H., and M. Murayama (2000), Radiocarbon of settling particles from hemipelagic region, *Nucl. Instrum. Methods Phys. Res., Sect. B*, *172*, 485–489.
Klaas, C., and D. E. Archer (2002), Association of sinking organic matter with various types of mineral ballast in the deep sea: Implications for the rain ratio, *Global Biogeochem. Cycles*, *16*(4), 1116, doi:10.1029/2001GB001765.
Lampitt, R. S., and A. N. Antia (1997), Particle flux in the deep seas: Regional characteristics and temporal variability, *Deep Sea Res., Part I*, *44*, 1377–1403.
Lamy, F., D. Hebbeln, and G. Wefer (1998), Terrigenous sediment supply along the Chilean continental margin: Modern regional patterns of texture and composition, *Geol. Rundsch.*, *87*, 477–494.
Lange, C. B., O. E. Romero, G. Wefer, and A. L. Gabric (1998), Offshore influence of coastal upwelling off Mauritania, NW Africa, as recorded by diatoms in sediment traps at 2195 m water depth, *Deep Sea Res., Part I*, *45*, 985–1013.
Lasaga, A. C., and H. Ohmoto (2002), The oxygen geochemical cycle: Dynamics and stability, *Geochim. Cosmochim. Acta*, *66*, 361–381.
Lee, C., et al. (1998), Particulate organic carbon fluxes: compilation of results from the 1995 US JGOFS Arabian Sea Process Study, *Deep Sea Res., Part II*, *45*, 2489–2501.
Lobbes, J. M., H. P. Fitznar, and G. Kattner (2000), Biogeochemical characteristics of dissolved and particulate organic matter in Russian Rivers entering the Arctic Ocean, *Geochim. Cosmochim. Acta*, *64*, 2973–2983.
Lohse, L., W. Helder, E. H. G. Epping, and W. Balzer (1998), Recycling of organic matter along a shelf-slope transect across the N.W. European Continental Margin (Goban Spur), *Prog. Oceanogr.*, *42*, 77–110.
Longhurst, A., S. Sathyendranath, T. Platt, and C. M. Caverhill (1995), An estimate of global primary production in the ocean from satellite radiometer data, *J. Plankton Res.*, *17*, 1245–1271.
Ludwig, W., J.-L. Probst, and S. Kempe (1996), Predicting the oceanic input of organic carbon by continental erosion, *Global Biogeochem. Cycles*, *10*, 23–41.
Luff, R., K. Wallmann, S. Grandel, and M. Schlüter (2000), Numerical modeling of benthic processes in the deep Arabian Sea, *Deep Sea Res., Part II*, *47*, 3039–3072.
Lyle, M., A. Mix, C. Ravelo, D. Andreasen, L. Heusser, and A. Olivarez (2000), Millennial-scale $CaCO_3$ and C-org events along the northern and central California margin: Stratigraphy and origins, *Proc. Ocean Drill. Program Sci. Results*, *167*, 163–182.
Manghnani, V., J. M. Morrison, T. S. Hopkins, and E. Boehm (1998), Advection of upwelled waters in the form of plumes off Oman during the Southwest Monsoon, *Deep Sea Res., Part II*, *45*, 2027–2052.
Matheron, G. (1965), *Les Variables Regionalisées et Leur Estimation*, Ed. Masson et Cie, Paris.
Meeuwis, J. M., and J. R. E. Lutjeharms (1990), Surface thermal characteristics of the Angola-Benguela Front, *S. Afr. J. Mar. Sci.*, *9*, 261–279.
Meggers, H., T. Freudenthal, S. Nave, J. Targarona, F. Abrantes, and P. Helmke (2002), Assessment of geochemical and micropaleontological sedimentary parameters as proxies of surface water properties in the Canary Islands region, *Deep Sea Res., Part II*, *49*, 3631–3654.
Meybeck, M. (1993), C, N, P and S in rivers: From sources to global inputs, in *Interactions of C, N, P and S: Biogeochemical Cycles and Global Change*, edited by R. Wollast et al., pp. 163–193, Springer-Verlag, New York.
Milliman, J. D., P. J. Troy, W. M. Balch, A. K. Adams, Y.-H. Li, and F. T. Mackenzie (1999), Biologically mediated dissolution of calcium carbonate above the chemical lysocline?, *Deep Sea Res., Part I*, *46*, 1653–1669.
Mollenhauer, G., R. R. Schneider, P. J. Müller, V. Spieß, and G. Wefer (2002), Glacial/interglacial variability in the Benguela Upwelling System: Spatial distribution and budgets of organic carbon accumulation, *Global Biogeochem.*, *16*, 1134, doi:10.1029/2001GB001488.
Mollenhauer, G., R. R. Schneider, T. Jennerjahn, P. J. Müller, and G. Wefer (2004), Organic carbon accumulation in the South Atlantic Ocean: Its modern, mid-Holocene and Last Glacial basin-wide distribution, *Global Planet. Change*, *40*, 249–266.
Murray, R. W., and M. Leinen (1996), Scavenged excess aluminum and its relationship to bulk titanium in biogenic sediment from the central equatorial Pacific Ocean, *Geochim. Cosmochim. Acta*, *60*, 3869–3878.
Neuer, S., V. Ratmeyer, R. Davenport, G. Fischer, and G. Wefer (1997), Deep water particle flux in the Canary Island region: Seasonal trends in relation to long-term satellite derived data and lateral sources, *Deep Sea Res., Part I*, *44*, 1451–1466.
OMEX-I (1997), Ocean Margin Exchange, OMEX-I project data set (1993–1994) [CD-ROM], Brit. Oceanogr. Data Cent., Bidston Observ., Birkenhead, UK.
Ovalle, A. R. C., C. E. Rezende, C. E. V. Carvalho, T. C. Jennerjahn, and V. Ittekkot (1999), Biogeochemical characteristics of coastal waters adjacent to small river-mangrove systems, East Brazil, *Geo Mar. Lett.*, *19*, 179–185.
Pace, M. L., G. A. Knauer, D. M. Karl, and J. H. Martin (1987), Primary production, new production and vertical flux in the eastern Pacific, *Nature*, *325*, 803–804.
Peinert, R., E. Bauerfeind, R. Gradinger, O. Haupt, M. Krumbholz, I. Peeken, I. Werner, and B. Zeitzschel (2001), Biogenic particle sources and vertical flux patterns in the seasonally ice-covered Greenland Sea, in *The Northern North Atlantic*, edited by P. Schäfer et al., pp. 69–79, Springer-Verlag, New York.
Peña, M. A., K. L. Denman, J. R. Forbes, S. E. Calvert, and R. E. Thomson (1996), Particle fluxes from the euphotic zone over the continental slope in an eastern boundary current region, *J. Mar. Res.*, *54*, 1097–1122.
Peña, M. A., K. L. Denman, S. E. Calvert, R. E. Thomsen, and J. R. Forbes (1999), The seasonal cycle in sinking particle fluxes off Vancouver Island, British Columbia, *Deep Sea Res., Part II*, *46*, 2969–2992.
Peña, M. A., K. L. Denman, and J. R. Forbes (2000), Shelf-ocean exchange water column and sediment trap data from the northeast Pacific, in *JGOFS Canada Data Sets 1989–1998* [CD-ROM], vers. 1.0, Mar. Environ. Data Serv., Dep. of Fish. and Oceans, Ottawa.
Peterson, R. G., C. S. Johnson, W. Krauss, and R. E. Davis (1996), Lagrangian measurements in the Malvonas Current, in *The South Atlantic: Present and Past Circulation*, edited by G. Wefer et al., pp. 239–247, Springer-Verlag, New York.
Pfannkuche, O., and K. Lochte (2000), The biogeochemistry of the deep Arabian Sea: Overview, *Deep Sea Res., Part II*, *47*, 2615–2628.
Prakash Babu, C., H.-J. Brumsack, and B. Schnetger (1999), Distribution of organic carbon in surface sediments along the eastern Arabian Sea: A revisit, *Mar. Geol.*, *162*, 91–103.
Ragueneau, O., et al. (2000), A review of the Si cycle in the modern ocean: Recent progress and missing gaps in the application of biogenic opal as a paleoproductivity proxy, *Global Planet. Change*, *26*, 317–365.
Ramseier, R., C. Garrity, E. Bauerfeind, and E. Peinert (1999), Sea-ice impact on long-term particle flux in the Greenland Sea's Is Odden-Nordbukta region, 1985–1986, *J. Geophys. Res.*, *104*, 5329–5343.
Rathburn, A. E., M. E. Perez, and C. B. Lange (2001), Benthic-pelagic coupling in the Southern California Bight: Relationships between sinking organic material, diatoms and benthic foraminifera, *Mar. Micropaleontol.*, *43*, 261–271.
Reimers, C. E. (1989), Control of benthic fluxes by particulate supply, in *Productivity of the Ocean: Present and Past*, edited by W. H. Berger et al., pp. 217–233, John Wiley, Hoboken, N. J.

Reimers, C. E., S. Kalhorn, S. R. Emerson, and K. H. Nelson (1984), Oxygen consumption rates in pelagic sediments from the Central Pacific: First estimates from microelectrode profiles, *Geochim. Cosmochim. Acta*, *48*, 903–911.

Reimers, C. E., R. H. Jahnke, and D. C. McCorkle (1992), Carbon fluxes and burial rates over the continental slope and rise off central California with implications for the global carbon cycle, *Global Biogeochem. Cycles*, *6*, 199–224.

Ritzrau, W., G. Graf, A. Scheltz, and W. Queisser (2001), Benthic-pelagic coupling and carbon dynamics in the northern North Atlantic, in *The Northern North Atlantic: A Changing Environment*, edited by P. Schäfer et al., pp. 207–224, Springer-Verlag, New York.

Romero, O., and C. Hensen (2002), Oceanographic control of biogenic opal and diatoms in surface sediments of the Southwestern Atlantic, *Mar. Geol.*, *186*, 263–280.

Rowe, G. T., G. S. Boland, W. C. Phoel, R. F. Anderson, and P. E. Biscaye (1994), Deep-sea floor respiration as an indication of lateral input of biogenic detritus from continental margins, *Deep Sea Res., Part II*, *41*, 657–668.

Sarnthein, M., J. Thiede, U. Pflaumann, H. Erlenkeuser, D. K. Fütterer, B. Koopmann, and H. E. S. Lange (1982), Atmospheric and oceanic circulation patterns off Northwest Africa during the past 25 million years, in *Geology of the Northwest African Continental Margin*, edited by U. Von Rad et al., pp. 584–604, Springer-Verlag, New York.

Sauter, E. J., M. Schlüter, and E. Suess (2001), Organic carbon flux and remineralization in surface sediments from the northern North Atlantic derived from pore-water oxygen microprofiles, *Deep Sea Res., Part I*, *48*, 529–553.

Schlesinger, W. H., and J. M. Melack (1981), Transport of organic carbon in the world's rivers, *Tellus*, *33*, 172–187.

Schlitzer, R. (2000), Electronic atlas of WOCE hydrographic and tracer data now available, *EOS Trans. AGU*, *81*, 45.

Schlitzer, R. (2002), Carbon export fluxes in the Southern Ocean: Results from inverse modeling and comparison with satellite-based estimates, *Deep Sea Res., Part II*, *49*, 1623–1644.

Schlüter, M., E. J. Sauter, A. Schäfer, and W. Ritzau (2000), Spatial budget of organic carbon flux to the seafloor of the northern North Atlantic (60°N–80°N), *Global Biogeochem. Cycles*, *14*, 329–340.

Schnetger, B., H.-J. Brumsack, H. Schale, J. Hinrichs, and N. Dittert (2000), Geochemical characteristics of deep-sea sediments from the Arabian Sea: A high-resolution study, *Deep Sea Res., Part II*, *47*, 2735–2768.

Seiter, K., C. Hensen, J. Schröter, and M. Zabel (2004), The organic carbon content in surface sediment: Defining regional provinces, *Deep Sea Res.*, in press.

Sirocko, F., D. Garbe-Schönberg, and C. Devey (2000), Processes controlling trace element geochemistry of Arabian Sea sediments during the last 25,000 years, *Global Planet. Change*, *26*, 217–303.

Smith, K. L. J., R. S. Kaufmann, and R. J. Baldwin (1994), Coupling of near-bottom pelagic and benthic processes at abyssal depths in the eastern North Pacific Ocean, *Limnol. Oceanogr.*, *39*, 1101–1118.

Smith, C. R., W. Berelson, D. J. Demaster, F. C. Dobbs, D. Hammond, D. J. Hoover, R. H. Pope, and M. Stephens (1997), Latitudinal variations in benthic processes in the abyssal equatorial Pacific: Control by biogenic particle flux, *Deep Sea Res., Part II*, *44*, 2295–2317.

Stein, R., and R. W. Macdonald (2003), Organic carbon budget: Arctic Ocean vs. global ocean, in *The Organic Carbon Cycle in the Arctic Ocean*, edited by R. Stein and R. W. MacDonald, pp. 315–322, Springer-Verlag, New York.

Suess, E. (1980), Particulate organic carbon flux in the oceans: Surface productivity and oxygen utilization, *Nature*, *288*, 260–263.

Takahashi, T., W. S. Broecker, and S. Langer (1985), Redfield ratio based on chemical data from isopycnal surfaces, *J. Geophys. Res.*, *90*, 6907–6924.

Thiede, J., G. W. Diesen, B. E. Knudsen, and T. Snare (1986), Patterns of Cenozoic sedimentation in the Norwegian-Greenland Sea, *Mar. Geol.*, *69*, 323–352.

Thomsen, C. (1993), Verfolgung pelagischer Prozesse mit Hilfe von biochemischen Komponenten am Beispiel der Alkenone (C37:2, C37:3), Ph.D. dissertation, Christian-Albrechts-Univ., Kiel, Germany.

Tintelnot, M. (1995), Transport and deposition of fine-grained sediments on the Brazilian Continental Shelf as revealed by clay mineral distribution, Ph.D. thesis, Ruprecht-Karls-Univ., Heidelberg, Germany.

Tribovillard, N. P., J.-P. Caulet, C. Vergnaud-Grazzini, N. Moureau, and P. Tremblay (1996), Lack of organic matter accumulation on the upwelling-influenced Somalia margin in a glacial-interglacial transition, *Mar. Geol.*, *133*, 157–182.

Tyson, R. V. (2001), Sedimentation rate, dilution, preservation and total organic carbon: Some results of a modelling study, *Org. Geochem.*, *32*, 333–339.

Uenzelmann-Neben, G. (1998), Neogene sedimentation history of the Congo Fan, *Mar. Pet. Geol.*, *15*, 635–650.

van Andel, T. H., G. R. Heath, and T. C. Moore (1975), Cenozoic history and paleoceanography of the central equatorial Pacific Ocean, *Geol. Soc. Am. Mem.*, *143*, 134.

van Bodungen, B., et al. (1995), Pelagic processes and vertical flux of particles: An overview of a long term comparative study in the Norwegian Sea and Greenland Sea, *Geol. Rundsch.*, *84*, 11–27.

van Camp, L., L. Nykjaer, E. Mittelstaed, and P. Schlittenhard (1991), Upwelling and boundary circulation off Northwest Africa as depicted by infrared and visible satellite observations, *Prog. Oceanogr.*, *26*, 357–402.

van der Weijden, C. H., G. J. Reichart, and H. J. Visser (1999), Enhanced preservation of organic matter in sediments deposited within the oxygen minimum zone in the northeastern Arabian Sea, *Deep Sea Res., Part I*, *46*, 807–830.

van Raaphorst, W., H. Malschaert, H. van Haren, W. Boer, and G.-J. Brummer (2001), Cross-slope zonation of erosion and deposition in the Faeroe-Shetland Channel, North Atlantic Ocean, *Deep Sea Res., Part I*, *48*, 567–591.

Wagner, T., M. Zabel, L. Dupont, J. Holtvoeth, and C. J. Schubert (2003), Terrigenous signals in sediments of the low latitude Atlantic—Implications for environmental variations during the late Quaternary, Part I: Organic carbon, in *The South Atlantic in the Late Quaternary: Reconstruction of Material Budget and Current Systems*, edited by G. Wefer et al., pp. 295–322, Springer-Verlag, New York.

Walsh, J. J. (1991), Importance of continental margins in the marine biogeochemical cycling of carbon and nitrogen, *Nature*, *350*, 53–55.

Walsh, J. J., D. A. Dieterle, and J. R. Pribble (1991), Organic debris on the continental margins: A simulation analysis of source and fate, *Deep Sea Res.*, *38*, 805–828.

Weaver, P. E., R. B. Wynn, N. H. Kenyon, and J. Evans (2000), Continental margin sedimentation, with special reference to the north-east Atlantic margin, *Sedimentology*, *47*, 239–256.

Wefer, G. (1989), Particle flux in the Ocean: Effects of episodic production, in *Productivity of the Oceans: Present and Past*, edited by W. H. Berger et al., pp. 139–153, John Wiley, Hoboken, N. J.

Wefer, G., and G. Fischer (1993), Seasonal patterns of vertical particle flux in equatorial and coastal upwelling areas of the Eastern Atlantic, *Deep Sea Res.*, *40*, 1613–1645.

Wenzhöfer, F., and R. Glud (2002), Benthic carbon mineralization in the Atlantic: A synthesis based on in situ data from the last decade, *Deep Sea Res., Part I*, *49*, 1255–1279.

Witte, U., and O. Pfannkuche (2000), High rates of benthic carbon remineralisation in the abyssal Arabian Sea, *Deep Sea Res., Part II*, *47*, 2785–2804.

Wollast, R. (1998), Evaluation and comparison of the global carbon cycle in the coastal zone and in the open ocean, in *The Sea*, edited by K. H. Brink and A. R. Robinson, pp. 213–252, John Wiley, Hoboken, N. J.

Wong, C. S., F. A. Whitney, D. W. Crawford, K. Iseki, R. J. Matear, W. K. Johnson, J. S. Page, and D. Timothy (1999), Seasonal and interannual variability in particle fluxes of carbon, nitrogen and silicon from time series traps at Ocean Station P, 1982–1993: Relationship to changes in subarctic primary productivity, *Deep Sea Res., Part II*, *46*, 2735–2760.

Wynn, R. B., D. G. Masson, D. A. V. Stow, and P. P. E. Weaver (2000), The northwest African slope apron: A modern analogue for deep water systems with complex seafloor topography, *Mar. Pet. Geol.*, *17*, 253–265.

Zabel, M., and H. D. Schulz (2001), Importance of submarine landslides for non-steady state conditions in pore water systems—Lower Zaire (Congo) deep-sea fan, *Mar. Geol.*, *176*, 87–99.

C. Hensen, GEOMAR - Forschungszentrum für Marine Geowissenschaften, SFB 574, Wischhofstraße 1-3, D-24148 Kiel, Germany.

K. Seiter and M. Zabel, Department of Geosciences, University of Bremen, Klagenfurter Straße, D-28359 Bremen, Germany. (kseiter@uni-bremen.de)